

Characterizing the effects of differentially adapted influenza PB2 proteins on duck MAVS-mediated interferon beta signaling

by

David Guy Tetrault

A thesis submitted in partial fulfillment of the requirements for the degree of

Master of Science

in

Physiology, Cell and Developmental Biology

Department of Biological Sciences
University of Alberta

© David Guy Tetrault, 2015

Abstract

The influenza A viral RNA polymerase is responsible for viral replication and greatly affects influenza A virus (IAV) virulence and host range. The PB2 influenza polymerase subunit is the primary polymerase determinant of influenza host range and virulence. It was previously shown that PB2 interacts with and inhibits MAVS-mediated interferon- β (IFN- β) expression to differing degrees depending on the localization of PB2 within mammalian cells. Specifically, mammalian adapted PB2 localized to the mitochondria while avian strains do not. This difference in localization was shown to be determined by a single amino acid difference in PB2. Here, I helped elucidate, in collaboration with the Sun Hur research group, the mechanism by which RIG-I activates MAVS-mediated IFN- β signaling. I subsequently determined that the PB2 proteins from 2 mammalian and 4 avian IAV strains differ in their abilities to inhibit duck MAVS-mediated IFN- β signaling in avian cells. Contrary to what was expected, mammalian adapted PB2 remained a potent inhibitor of avian IFN- β signaling despite major differences between human and duck MAVS. Additionally, swapping the adaptive PB2 residue 9, between avian and human adapted IAV strains, did not affect the general pattern of PB2-mediated IFN- β inhibition. Although, changes in PB2-MAVS interactions and PB2 localization were observed. My results demonstrate that the PB2 inhibition of IFN- β in avian cells is partially dependent on PB2-MAVS interactions and PB2 localization. Together, these findings suggest mammalian IAV PB2 proteins have acquired a cross species ability to inhibit IFN- β signaling, which has the potential to affect both IAV virulence and fitness.

Importance

During an influenza virus infection, IFNs are produced through MAVS-mediated signaling, creating an antiviral state within the host cell. IFN then works to limit IAV replication within the host, which has an effect on viral transmission and fitness. Avian adapted IAVs are capable of reaching high rates of replication and transmission in ducks. However, very few avian adapted IAVs can transmit efficiently between humans. I wondered whether this was partially due to specific adaptations in IAV PB2 proteins that restricted PB2 inhibition of MAVS-mediated IFN signaling to specific hosts. Surprisingly, I have shown that mammalian adapted IAV PB2 has acquired the cross species ability to be a potent IFN inhibitor in avian cells. Here I have begun to characterize how this IFN inhibition is mediated, as it is important to comprehend the mechanisms that influenza uses to adapt and improve viral fitness in new hosts.

Preface

Some of the data presented in this thesis is from a research collaboration, led by Associate Professor Sun Hur at the Harvard Medical School, and Professor Katharine Magor, the lead collaborator at the University of Alberta. The collaborative data discussed in this thesis has been published as Wu B., Peisley A., Tetrault D., Li Z., Egelman E.H., Magor K.E., Walz T., Penczek P.A., Hur S., “Molecular imprinting as a signal-activation mechanism of the viral RNA sensor RIG-I,” 2014, *Molecular Cell*, vol. 55, issue 4, 511-523.

The results in Figures 6 and 7 have been taken from the published work above, and the discussion of these results has been described in my own words in chapters 3.1, 3.2, 4.1, and 4.2. The functional assays performed to quantify the chicken IFN- β promoter activity in DF-1 cells (Figure 6 and 7), were performed by myself. All other data presented in figures 6 and 7 was published as previously stated. The wild type duck MAVS and duck MAVS-V5 expression constructs were both created by myself, however all other mutant MAVS and RIG-I constructs presented in Figures 6 and 7 were supplied by the Sun Hur research group. The introduction in Chapter 1, materials and methods in chapter 2, the additional results in chapter 3, and the discussion in chapter 4 outside of what has been mentioned is my original work.

Acknowledgements

I would like to first thank my supervisor, Dr. Katharine Magor, for all the support and guidance you have given me throughout my academic career. I owe it to you for sparking my interest in research and immunology during my time as an undergraduate student in your Immunology 200 class, all those years ago. Since then, you have provided me with every opportunity to succeed as both an academic and professional. I have learned so much under your guidance. You have helped develop my research and professional skills during my time in your lab. I look forward to using these skills to aid me in becoming the best medical professional I can be.

Thank you to my committee members, Dr. James Stafford and Dr. Bart Hazes. I cannot thank you enough for all the time, support, and technical skills you have provided me with over my two years as a graduate student. Your effort has not gone unnoticed.

I would also like to recognize all the lab members from the Magor lab for being very supportive. Domingo and Ximena you provided me with most of my technical skills, I knew very little when I first started in the lab. I would also like to thank Graham for your help with florescence work and Danyel for all your protein work expertise. Thank you Luke for your help in troubleshooting the very difficult cloning of PB2. Thank you Eleya, Dustin, Myron, Jeff, Jordan, Alexa, Eric, Alysson and anyone I missed, as your support and friendship made my time as a graduate student very enjoyable.

I would also like to thank my funding sources. I was financially funded by the Department of Biological Sciences, GSA, FGSR, and the QEII scholarship during my degree.

Last but not least, I would like to thank my family. Thank you Carmen, for all the support and editing help, and for being the best sister a brother could ask for. Thank you to Guy and Donna for being the most supportive parents. I could not have completed two degrees, going on three, without your help and support. I owe it to you for instilling in me a great work ethic and dedication to family. Thank you to my partner Fiona, I met you before I started this journey, and I could not have done it without you. Thank you for the loving support, friendship, and encouragement.

Table of Contents

| | |
|--|----|
| Chapter 1. Introduction | 1 |
| 1.1 Influenza A virus biology | 1 |
| 1.1.1 Influenza A genome organization | 1 |
| 1.1.2 Influenza A replication cycle | 2 |
| 1.2 Wild waterfowl and influenza A viruses | 4 |
| 1.3 Mammalian adaptive influenza A mutations | 6 |
| 1.3.1 Hemagglutinin (HA) | 6 |
| 1.3.2 Neuraminidase (NA) | 8 |
| 1.3.3 Non-structural protein 1 (NS1) | 8 |
| 1.4 The influenza A polymerase | 10 |
| 1.5 Influenza A polymerase determinants of host adaptation | 10 |
| 1.6 Intracellular detection of influenza viral RNA | 11 |
| 1.7 PB2-MAVS interactions | 12 |
| 1.8 Experimental aims and results summary | 13 |
| 1.8.1 Experimental aims | 14 |
| Chapter 2. Materials and Methods | 18 |
| 2.1 Viruses | 18 |
| 2.2 Cloning and Plasmids | 18 |
| 2.3 IFN- β reporter assays in collaboration with Sun Hur | 20 |
| 2.4 PB2 protein structure modeling and alignment | 21 |

| | |
|---|----|
| 2.5 Immunoprecipitation and Western blotting | 22 |
| 2.6 IFN- β reporter assays for PB2 and MAVS | 23 |
| 2.7 Fluorescent microscopy and localization analysis | 23 |
| Chapter 3. Results | 32 |
| 3.1 A T175/T176 mutation in duck 2CARD ^{RIG-I} enables IFN signaling in human cells. | 32 |
| 3.2 Mutations at residues 43 and 56 in both duck and human MAVS abrogates MAVS- mediated IFN signaling. | 33 |
| 3.3 Modeling influenza PB2 illustrates three human adaptive residues near the PB2 MAVS binding domain. | 34 |
| 3.4 Not all avian influenza PB2 can bind to duck MAVS. | 35 |
| 3.5 The PB2 mutation D9N in the LPAI M546 strain restores duck MAVS binding. | 35 |
| 3.6 Mammalian IAV PB2 proteins are potent inhibitors of duck MAVS IFN- β signaling. | 36 |
| 3.7 Mammalian adapted PB2 shows partial localization with duck MAVS in avian cells. | 37 |
| 3.8 A PB2 mutation at residue 9 causes increased cytoplasmic staining of HPAI and mammalian adapted PB2 proteins. | 38 |
| 3.9 Mammalian adapted IAV PB2 proteins have increased non-nuclear staining that is not dependent on residue 9. | 39 |
| Chapter 4. Discussion | 50 |
| 4.1 The RIG-I-MAVS filament nucleation event is transient. | 50 |
| 4.2 MAVS filament formation is conserved across species. | 51 |
| 4.3 Influenza PB2 inhibition of MAVS IFN signaling | 52 |
| 4.4 Mammalian adapted PB2 is a potent cross species inhibitor of IFN- β | 52 |

| | |
|---|----|
| 4.5 PB2 displays three adaptive residues, which form a cleft like structure near the MAVS binding domain..... | 54 |
| 4.6 PB2-mediated IFN inhibition is partially dependent on PB2-MAVS interactions..... | 55 |
| 4.7 PB2-mediated IFN inhibition is partially dependent on PB2 localization..... | 57 |
| 4.8 PB2-mediated IFN inhibition could increases viral fitness for mammalian adapted IAVs. | 59 |
| 4.9 Conclusions | 61 |
| References..... | 63 |

List of Figures

| | |
|---|----|
| Figure 1. Graphical representation of the RIG-I-MAVS signaling pathway..... | 17 |
| Figure 2. Vector map of pcDNA3.1/Hygro+ with a duck MAVS insert..... | 27 |
| Figure 3. The effect of duck MAVS and duck MAVS-V5 on the chicken IFN- β promoter activity. | 28 |
| Figure 4. Vector map of pSMART-CMV with an influenza A PB2 insert. | 29 |
| Figure 5. Flow chart depicting the method in which the pSMART-CMV expression vector was generated. | 30 |
| Figure 6. Analysis of the 2CARD ^{RIG-I} :CARD ^{MAVS} interface. | 41 |
| Figure 7. Analysis of the CARD interface within the MAVS filament..... | 42 |
| Figure 8. Map of adaptive residues within the PB2 structure..... | 43 |
| Figure 9. Analysis of PB2-MAVS protein interactions..... | 44 |
| Figure 10. PB2 inhibition of MAVS-mediated IFN signaling..... | 45 |
| Figure 11. Localization of PB2 and MAVS within DF-1 cells..... | 47 |
| Figure 12. Localization of PB2 and DF-1 cell mitochondria..... | 48 |
| Figure 13. Percent non-nuclear PB2 staining in DF-1 cells..... | 49 |

List of Tables

| | |
|--|----|
| Table 1. Primer sequences for amplification of duck MAVS and IAV PB2s. | 25 |
| Table 2. Primer sequences for sequencing of duck MAVS and IAV PB2s..... | 26 |
| Table 3. Primer sequences for amplification of the CMV promoter from pcDNA3.1/Hygro+.... | 31 |

Abbreviations

| | |
|--------|--|
| BC500 | A/Dk/British Columbia/500/2005 (H5N2) |
| CARD | Caspase activation and recruitment domain |
| CPSF30 | Cleavage and polyadenylation specificity factor 30 |
| D4AT | A/Dk/D4AT/71.1/2004 (H5N1) |
| DF-1 | Spontaneously immortalized chicken embryonic fibroblasts cells |
| DMEM | Dulbecco's modified eagle medium |
| FBS | Fetal bovine serum |
| HA | Hemagglutinin |
| HPAI | Highly pathogenic avian influenza |
| IAV | Influenza A virus |
| IB | Immunoblot |
| IFN | Interferon |
| IP | Immunoprecipitation |
| ISG | Interferon stimulated gene |
| LPAI | Low pathogenic avian influenza |
| LRT | Lower respiratory tract |
| M1 | Influenza Matrix protein 1 |
| M2 | Influenza Matrix protein 2 |
| M546 | A/duck/Memphis/546/1974(H11N9) |
| MAVS | Mitochondrial antiviral signaling protein |
| MBCS | Multibasic cleavage site |
| MCS | Multiple cloning site |

| | |
|---------|---|
| MDA5 | Melanoma Differentiation-Associated protein 5 |
| NA | Neuraminidase |
| NEP/NS2 | Nuclear export protein/Non-structural protein 2 |
| NLS | Nuclear localization signal |
| NP | Nucleoprotein |
| NS1 | Non-structural protein 1 |
| PA | Polymerase acidic protein |
| PB1 | Polymerase basic protein 1 |
| PB2 | Polymerase basic protein 2 |
| PCR | Polymerase chain reaction |
| PR8 | A/Puerto Rico/8/1934 (H1N1) |
| PRR | Proline rich region |
| RIG-I | Retinoic Acid Inducible Gene-I |
| RNA | Ribonucleic acid |
| RNP | Ribonucleoprotein |
| SA | Sialic acid |
| TRAF | Tumor necrosis factor receptor associated factor family |
| URT | Upper respiratory tract |
| VN1203 | A/Vietnam/1203/2004 (H5N1) |
| X31 | A/X-31/2003 (H3N2) |

Chapter 1. Introduction

1.1 Influenza A virus biology

1.1.1 Influenza A genome organization

Influenza A viruses (IAV) are enveloped RNA viruses belonging to the family *Orthomyxoviridae*, which are characterized by a negative-sense, single-stranded, segmented RNA genome (reviewed in [1]). The segmented genome of IAVs is composed of 8 segments, which express several different proteins. Traditionally, the largest RNA segments, 1 through 3, encode the three subunits of the IAV polymerase, polymerase basic protein 2 (PB2), polymerase basic protein 1 (PB1), and polymerase acidic protein (PA) (reviewed in [2]). These polymerase subunits together with the IAV nucleoprotein (NP), encoded by segment 5, make up the ribonucleoprotein (RNP) complex, which is contained within the virion core. Segments 4 and 6 encode for the exterior glycoproteins, hemagglutinin (HA) and neuraminidase (NA), which are embedded within the host cell-derived membrane envelope. The envelope also contains the viral ion channel protein, matrix protein 2 (M2), which is encoded by segment 7. The viral envelope surrounds the virion core, which is composed of matrix protein 1 (M1) encoded by segment 7. Within the core, segment 8 encodes for the nuclear export protein (NEP/NS2). Only the non-structural protein 1 (NS1), encoded by segment 8, is not found within the virion core (reviewed in [2]).

In more recent studies, the number of identified IAV proteins has grown. Segment 2 has been found to express two similar PB1 like proteins PB1-F2 and PB1-NP40. PB1-F2 is expressed from the second open reading frame from the PB1 gene, and it is found to be a trigger of

proapoptotic function and increased IAV pathogenicity in mice (3). While PB1-NP40 is composed of the N-terminal 39 residues of PB1, and is found to affect IAV replication (4). Additionally, segment 3 has been identified to express three novel PA related peptides, PA-X, PA-N155, and PA-N182. All three of the PA related peptides do not exhibit polymerase activity, however mutant IAVs which lack any one of these novel peptides display a decrease in viral replication and virulence (5, 6). More recently, a 10 kDa PB2 related protein, sharing the N-terminal portion of PB2, has been identified (7). This truncated PB2 has been implicated in inducing the expression of interferon- β (IFN- β), an effect that is the exact opposite of full length PB2 (8, 9). Together, the genomic segments of IAVs encode for several viral proteins during infection. Most of the primary functions of these viral proteins are known, however novel proteins and functions are discovered annually and represent a large area of IAV research.

1.1.2 Influenza A replication cycle

IAVs use sialic acids on the surface of host cells as receptors to trigger viral entry (10). It is the viral HA protein that mediates the interaction with specific host sialic acid receptors. After binding, IAVs are primarily internalized through clathrin-mediated endocytosis (11). Once internalized, a drop in pH within the endosome causes conformational changes to the HA structure, exposing the IAV fusogen. This allows for the fusion of the viral envelope to the host endosomal membrane, creating an endosomal pore (reviewed in [12]). At the same time, the M2 viral ion channels are also lowering the pH within the IAV virion. This disrupts protein-protein interactions and releases the RNPs from the M1 proteins in the acidified virion, allowing for the delivery of the freed RNPs through the newly opened endosomal pore to the cytoplasm (13).

RNPs are then translocated to the nucleus via their nuclear localization signals (NLS), which instruct cellular host proteins to import the viral RNPs to the nucleus (reviewed in [14]).

The nucleus is where IAV mRNA synthesis and replication occurs (reviewed in [1]). The IAV RNA-dependent RNA polymerase, a component of the RNP complex, is composed of PB1, PB2, and PA. The IAV polymerase uses viral negative sense ss-RNA to synthesize both viral mRNA for viral protein expression and full-length RNA copies for packaging into new IAV virions. To initiate transcription, the IAV polymerase interacts with the host polymerase II (15), which allows for the PB2 and PA viral polymerase subunits to steal the 5' cap from host pre-mRNA in a process known as “cap snatching” (16, 17). Once capped and polyadenylated, the newly synthesized mature viral mRNAs are then exported and translated like any other host mRNA to create viral proteins. The newly copied full-length viral RNA segments then assemble with NP and the viral polymerase subunits, creating new RNPs. The RNPs are then exported from the nucleus to the cytoplasm through interactions with M1 and NEP (18, 19).

Assembly of new IAV virions occurs in lipid rafts on the apical side of the cell surface, where M1 matrix protein begin to accumulate (20). Signals for the association of HA and NA directs the IAV glycoproteins to the lipid rafts (21). RNPs then translocate to the site of assembly within the lipid rafts, where interactions with M1 and plasma membrane initiate budding (22). After budding, HA keeps the virion anchored to the cell membrane via interactions with the host sialic acid receptors, consequently NA is required for the release of the virion by cleaving surface sialic acid molecules from the host cell (23). After release, the newly synthesized viral particles continue on to repeat the infection cycle described above.

1.2 Wild waterfowl and influenza A viruses

IAVs are classified into subtypes based on the antigenic properties of their HA and NA surface glycoproteins. Currently there are 18 HA subtypes (H1-H18) and 11 NA subtypes (N1-N11) known to exist within the IAV population (24). The combination of any one HA subtype with any other NA subtype provides the information needed to name the subtype of an IAV, for example H1N2. Almost all IAV subtypes have been shown to circulate in wild waterfowl and therefore wild aquatic birds (ducks) are long thought to be the natural reservoir of IAVs (25). H17-18 and N10-11 are the only subtypes that have not been shown to circulate in wild birds, as these subtypes were recently discovered in wild bat samples (24). Avian IAVs usually replicate asymptotically in the intestinal tract of ducks and are excreted in high volumes into the environment via fecal contaminated pond water (26). IAV infection can then spread from the natural host to several other species such as swine, poultry, and humans. In humans however, only the H1-H3 and N1-N2 subtypes of IAV have been able to circulate with regularity and are capable of causing severe pathologies (27).

Avian IAVs can be further subdivided into two categories, low pathogenic avian influenza (LPAI) and high pathogenic avian influenza (HPAI). The designation of pathogenicity is based on two criteria laid out by the World Organization for Animal Health (OIE). Firstly, HPAI must exhibit a certain level of pathogenicity in 4-8 week-old chickens, where either 75% mortality is caused within 10 days, or the inoculation of 10 susceptible 6-week-old chickens results in an intravenous pathogenicity index greater than 1.2 (28). Secondly, regardless of chicken pathogenicity, any IAV that displays a similar HA amino acid sequence to an H5 or H7 virus containing the multibasic cleavage site (MBCS), will be considered a HPAI as well.

Wild waterfowl are fundamentally important to the worldwide spread of IAVs, due to the sheer geographic distance that migratory birds can cover (29). Ducks and other wild waterfowl are known to have the broadest IAV subtype variety and highest IAV prevalence rates, thus providing an ideal vessel to harbor a genetically diverse IAV gene pool. A gene pool, which yields the capability of producing highly pathogenic and pandemic influenza strains in other species (25). In humans, four IAV strains have caused pandemics within the last century, all of which have been caused by IAVs with avian genetic origins. The 1918 ‘Spanish’ influenza pandemic was caused by an H1N1 IAV strain, which is thought to have evolved from an avian adapted IAV in 1910 (30). The 1918 pandemic is known as the deadliest pandemic in recorded history, as it killed an estimated 50 million people worldwide (31). The ‘Asian’ influenza pandemic then occurred 39 years later, in 1957, and was caused by an H2N2 IAV. Although not as lethal, it is estimated to have caused 2 million deaths worldwide (32), and originated from the combination of a circulating H1N1 and an avian adapted H2N2 IAV (33). About 10 years later, the ‘Hong Kong’ H3N2 IAV pandemic replaced the circulating H2N2 viruses in 1968 and caused about 1 million deaths worldwide (32). The H3N2 pandemic is thought to have been caused by a reassortment event between an avian H3 virus and the circulating human H2N2 IAV (33). Finally, the most recent pandemic was caused by the 2009 H1N1 IAV. Within the first year, it is estimated that the 2009 H1N1 pandemic caused an estimated 151 700 to 575 400 deaths worldwide (34). However, unlike the other pandemics, the 2009 IAV originated from a reassortment event between a Eurasian swine IAV and a triple reassortant human, swine, and avian IAV (35). Taken together, these pandemics demonstrate that avian reservoirs can harbor IAVs that contain the genetic traits that are favorable for increases in transmission and

pathogenicity in mammals. Interestingly however, these avian related viruses display limited pathology in wild birds (25). Thus, to help explain these differences and help identify future human IAV strains with pandemic potential, it is important to characterize the adaptive genetic changes that are associated with increased IAV virulence and host specificity in humans.

1.3 Mammalian adaptive influenza A mutations

1.3.1 Hemagglutinin (HA)

Initially, the HA IAV protein is translated as an inactive polypeptide precursor (HA0) and must be cleaved into the HA1 and HA2 domains for functionality to be attained. The number of basic residues within the HA cleavage site determines which cellular proteases can activate HA. LPAI strains only display a single basic residue that can be cleaved by trypsin-related enzymes, which are restricted to the intestinal and respiratory tracts of birds (36). Conversely, HPAI viruses such as H5 and H7 subtypes contain a MBCS, which can be cleaved by multiple and more ubiquitous cellular proteases, and thus they are not limited to replicating in certain tissues (37). Although the association of HA cleavability and systemic infection is well correlated in avian IAV infections, this correlation does not show the same phenotype in mammals. Recently, studies have found that the depletion of the MBCS in the H5N1 HPAI results in decreased viral replication that is restricted to the respiratory tract in ferrets (38, 39). However, the addition of the MBCS does not necessarily confer the ability to replicate systemically, as a mammalian H3N2 virus with an added MBCS could not initiate a systemic infection in ferrets (40). Therefore, it appears that virulence, replication, and most likely transmission in mammalian

adapted IAVs are affected by a MBCS in HA. However, it appears there are several other HA factors that determine IAV adaptation to mammals.

As discussed previously, IAV HA is responsible for initiating viral entry by interacting with host cell surface sialic acid (SA) receptors (10). It is known that human adapted IAVs preferentially interact with SA receptors that display an α 2,6-glycosidic bond (SA- α 2,6), while avian adapted IAVs prefer an α 2,3-glycosidic bond (SA- α 2,3). Consequently, this determines where adapted IAVs can replicate, as the SA- α 2,6 is predominantly expressed in the upper respiratory tracts (URT) of humans, and the SA- α 2,3 is expressed in avian intestinal epithelium and the lower respiratory tracts (LRT) of humans. In humans, URT binding and replication is thought to correlate strongly with increased human IAV transmission, as it increases the possibility for IAVs to transmit via aerosol droplets. Specifically, the SA receptor specificity of HA is determined by amino acid residue substitutions in the receptor binding domain of HA. Briefly, the residue substitution Q226L in H2 and H3 IAV subtypes has been shown to change the HA binding specificity from avian to human SA receptors (reviewed in [41]). Yet, some IAV subtypes have displayed dual receptor binding capabilities between avian and mammalian SA receptors. The novel H7N9 IAV subtype has displayed HA binding capabilities for both the SA- α 2,6 and SA- α 2,3 receptors (42), granting H7N9 IAVs the ability to attach in both the LRT and URT in humans. To date, some H5N1 IAVs have also displayed this dual SA receptor attachment; however, both H7N9 and H5N1 viruses primarily replicate in the LRT of humans, which correlates with increased virulence in humans (43). Therefore, it can be reasoned that adaptive HA mutations that increase IAV binding to human URT SA receptors, would increase

transmission but at the cost of possibly decreasing virulence. This is a trade-off that directly affects viral fitness in new hosts.

1.3.2 Neuraminidase (NA)

While HA is required for IAV binding and entry, the IAV NA is required for the release of progeny IAV virions from an infected cell. It accomplishes this by cleaving surface sialic acid molecules from the infected host cells, to allow for efficient release of viral particles in an infected host (23). Since HA and NA have competing functions during an IAV infection by either binding or cleaving SA receptors, a balance must be achieved between these two viral activities (44). Changes in IAV NA cleavage activities can affect viral replication or virulence, and thus be a determinate of host adaptation. An H7N7 HPAI virus in chickens had caused an outbreak in humans in 2003, which killed one individual and infected 89 others (45). Upon investigating the differences between the lethal and non-lethal H7N7 isolates, it was found that four NA mutations had occurred, which increased the NA activity and improved replication in mammalian cells by reducing the formation of IAV aggregates (46). Along with these mutations, NA deletions that shorten the NA stalk length have also been shown to increase virulence in mammalian hosts infected with H5N1 IAVs (47). However, how a shorter NA contributes to virulence and subsequent IAV host adaptation is poorly understood and represents a current field of research.

1.3.3 Non-structural protein 1 (NS1)

The primary function of the IAV NS1 is to inhibit the antiviral IFN response in infected cells (reviewed in [48]). Due to this IFN inhibition, NS1 is known to be an important molecular determinant of IAV virulence and host range. Previously, research has shown that IAV viruses

which lack NS1 are only able to replicate in mice or cells where the IFN response is compromised (49). This indicates that NS1 plays a crucial role in modulating the host innate immune defenses. Specifically, NS1 is known to inhibit cellular gene expression of key antiviral interferon stimulate genes (ISGs) by preventing the processing of cellular mRNAs. One way NS1 inhibits cellular gene expression is by binding to CPSF30, a cellular factor that is involved in pre-mRNA processing (50). Interestingly, CPSF30-NS1 binding is not conserved between all strains of IAVs. In fact, several NS1 residue mutations in the H5N1 IAV have been shown to increase NS1 binding to CPSF30, which has in turn increased viral replication (51). However, it is important to note that CPSF30 and NS1 binding is not the sole determinant of IAV virulence or replication. Research has shown that restoring NS1-CPSF30 binding in the H1N1 2009 pandemic virus did not affect viral virulence in several animal models (52).

In summary of the literature, it is evident that there are several crucial mutations that allow for IAVs to infect humans. However, none of these human adaptive IAV mutations can function independently to determine host specificity and virulence. Rather, host specificity and virulence is most likely determined by a multiplicity of factors that work co-operatively to allow IAVs to jump the species barrier. This then demonstrates the importance to characterize all the molecular interactions between the virus and host that dictate viral pathogenicity and host range. In the case of IAVs, this knowledge is invaluable with regards to disease prevention, since it can yield potential drug targets and better surveillance strategies to help identify IAV strains with pandemic potential in humans (53). To date, some of these adaptive mutations have been described to occur within the IAV polymerase.

1.4 The influenza A polymerase

As previously described, the IAV polymerase is responsible for the transcription and replication of IAVs. The IAV polymerase is composed of three subunits, PA, PB1, and PB2. PA is known to function as an endonuclease and protease, while also contributing to vRNA promoter binding (54–56). PB1 houses the viral polymerase active site (57), and also forms the core of the IAV polymerase by interacting with both PA and PB2 (58, 59). PB2 contains the cap-binding domain that is responsible, in combination with PA, for stealing the 5' cap from host pre-mRNA molecules in a process known as “cap snatching” (16, 17). Furthermore, PB2 also contains a bipartite nuclear localization signal that allows it to be transported to the nucleus independently of PA and PB1 (60, 61). Together, all three polymerase subunits are required for proper polymerase function, however several possible molecular determinants of IAV pathogenicity and host adaptation have been identified within each polymerase subunit (62).

1.5 Influenza A polymerase determinants of host adaptation

IAV virulence is impacted by all three polymerase subunits, however PB2 is the primary polymerase determinant of IAV virulence and host specificity (27). A major factor in interspecies transmission between different IAV strains is the ability to adapt to different importin- α proteins (63), as these vary greatly between avian and mammalian species. Importin- α is important to IAVs because it is responsible for translocating released viral RNPs to the nucleus in order to continue the IAV infection. Specifically, a D701N mutation in an avian IAV PB2 protein conferred enhanced importin- α binding and increased PB2 nuclear localization in mammalian cells (64). It is thought that this mutation greatly improves the efficiency of the IAV polymerase in mammalian cells by more directly targeting PB2 to the nucleus. Furthermore,

several other PB2 mutations (E627K, G590S/Q591R) have been demonstrated to improve the avian IAV polymerase activity in mammalian cells (65, 66). The E627K mutation is found in most human adapted IAVs, as a lysine at position 627 confers the ability for the virus to replicate in the URT of mammals (67). This was found to be due to the temperature of the URT, since the avian E627 residue restricts viral replication at this lower temperature. Together, these findings have identified several mutations within PB2 that have allowed IAVs to adapt to humans. However, more recent studies have focused on the capability of PB2 to inhibit the IFN- β response during IAV infection (8, 9).

1.6 Intracellular detection of influenza viral RNA

RNA viruses, like influenza, are typically detected early during infection by the innate immune cytosolic receptors RIG-I and MDA5 (68). These receptors then activate the innate immune response by stimulating the production of Type-I IFNs, which create an antiviral state by upregulating several ISGs in neighbouring host cells. Retinoic Acid-Inducible Gene (RIG-I) and Melanoma Differentiation-Associate Gene 5 (MDA5) share similar domain composition, consisting of two tandem N-terminal caspase activation and recruitment domains (2CARD), a central helicase domain and a C-terminal domain that all function cooperatively to recognize specific viral RNA motifs (69). Although RIG-I and MDA5 share similar structures and downstream signaling pathways through the mitochondrial antiviral signaling protein (MAVS), they still detect largely different groups of viruses due to their RNA binding specificity (70). RIG-I has been found to bind 5'-triphosphate ss-RNA molecules that are produced during IAV infection (71). However, the molecular mechanism for how active RIG-I interacts with the downstream adaptor protein MAVS, to propagate the IFN signaling pathway remained uncharacterized until recently (72).

Normally, RIG-I is found in an auto-suppressed state in the absence of a viral infection by binding the helicase domain to the intramolecular 2CARD (2CARD^{RIG-I}) (73). Upon the binding of viral RNA to the RIG-I helicase domain, the 2CARD^{RIG-I} is released and forms a homotetramer with the neighbouring free 2CARD^{RIG-I}, as seen in Figure 1 (74). The 2CARD^{RIG-I} tetramer then interacts with the lone N-terminal CARD from MAVS (CARD^{MAVS}) to form self-perpetuating MAVS filaments. These filaments bring several proline rich regions (PRR) of MAVS together that then act as a scaffolding or docking site for several downstream adaptor proteins, which are necessary to propagate the antiviral signal to produce Type-I interferons (IFNs) (75, 76). The RIG-I-MAVS antiviral signaling pathway is crucial to initiating an antiviral defense and because of this, it is often a target of viral proteins, such as the IAV PB2 protein. Therefore, it is important to characterize the mechanism of MAVS signaling and begin to understand how viral proteins such as the PB2 can interact and inhibit the MAVS IFN-signaling.

1.7 PB2-MAVS interactions

As previously described, PB2 is known to localize to the nucleus of infected cells to help form the IAV polymerase. Conversely, PB2 has also been described to localize with the mitochondria of host cells (77, 78). In more recent studies, it was shown that this mitochondrial localization of PB2 was related to interactions with the host MAVS protein (8). Interestingly, PB2 from differentially adapted IAVs displayed varied localization patterns within mammalian cells. It was determined that the PB2 mitochondrial localization was caused by a single residue change within the PB2 protein at position 9. Specifically, mammalian adapted IAV PB2 proteins (N9) co-localized with the mitochondria, while avian adapted IAV PB2 proteins (D9) did not. This variance in PB2-MAVS co-localization also caused differences in the ability of PB2 to inhibit

MAVS-mediated IFN- β signaling (8, 9). Mammalian adapted PB2 was found to be a more potent inhibitor of human MAVS IFN- β signaling than avian adapted PB2. This is very interesting as it was the first reported case of PB2 directly interfering with an IFN signaling response. Additional research then characterized which part of PB2 mediated this MAVS interaction. It was determined that the first 37 N-terminal residues of PB2 along with the CARD and PRR domains of MAVS mediated the PB2-MAVS interaction in humans (79). To date, it is known that residue 9 of PB2 is a transmissibility factor that determines the adaptation of IAVs to human hosts (80). However, it is currently unknown how this adaptive mutation affects the function of PB2 in the natural host, ducks.

1.8 Experimental aims and results summary

Studies have shown that mammalian adapted PB2 inhibits IFN- β signaling in mammalian cells to a greater extent than avian adapted PB2 by interacting with mammalian MAVS (8, 9). This is caused by an adaptive mutation in PB2 at position 9 that has been shown to control PB2 mitochondrial localization. It is currently unknown how this adaptive mutation affects the function of IAV PB2 in the natural host, ducks. Therefore, it is hypothesized, that differences in IFN inhibition between mammalian and avian adapted IAV PB2, stems from the selective pressure for PB2 to interact with specific MAVS molecules to improve viral fitness. MAVS from the natural IAV host, ducks, is only ~25% identical to human MAVS, and thus the avian IAV PB2 should be better adapted than mammalian PB2 to inhibit and interact with duck MAVS. Here, I collaborated with Sun Hur to determine the structural mechanism of RIG-I-MAVS activation. I have also demonstrated that PB2 proteins from 2 mammalian and 4 avian adapted IAV strains differ in their ability to inhibit duck MAVS-mediated IFN- β signaling in avian cells. Unexpectedly, mammalian adapted IAV PB2 is found to be a more potent inhibitor of avian IFN-

β signaling, as compared to avian adapted PB2. Additionally, swapping the adaptive PB2 residue 9, between avian and mammalian adapted influenza strains, did not affect the general pattern of PB2-mediated IFN- β inhibition, although changes in PB2-MAVS interactions and PB2 localization were observed. With these results, I demonstrate that the mammalian IAV PB2 has most likely adapted to be a potent cross species inhibitor of avian IFN- β signaling, a function that is partially dependent on both PB2-MAVS interactions and PB2 cellular localization.

1.8.1 Experimental aims

Aim 1. Test specific MAVS and RIG-I mutations to test the Sun Hur model of RIG-I-MAVS signal activation.

The Sun Hur research group's crystal structure and proposed model of RIG-I-MAVS signal activation provided a novel mechanism for how RIG-I IFN signaling is achieved (74, 81). In a collaborative effort to test their work within an avian model, I tested several of their generated duck RIG-I and MAVS constructs in avian DF-1 cells. I provided cloned duck MAVS and Sun Hur selected and made mutations in both duck RIG-I and MAVS based on their ability to abrogate and restore IFN- β signaling, as predicted from the RIG-I-MAVS crystal structure. I established a dual luciferase assay system to analyze the chicken IFN- β promoter activity after transfection with duck RIG-I and MAVS constructs in DF-1 cells.

Aim 2. Identify potential IAV strain specific residues responsible for differences in PB2 function.

IAV PB2 proteins from 4 avian adapted strains and 2 mammalian adapted strains were cloned, sequenced, and analyzed for residue differences near the MAVS binding domain of PB2. PB2 from PR8 was modeled on a known IAV PB2 crystal structure to obtain structural information on where certain known adaptive residues were located within the PB2 structure.

Aim 3. Examine the protein interactions between duck MAVS and differently adapted IAV PB2 proteins.

PB2 is thought to interact with MAVS to inhibit the IFN response in human cells. Differences in PB2-MAVS interactions could explain variation in PB2-mediated IFN inhibition. PB2 and duck MAVS expression vectors were co-transfected in DF-1 chicken fibroblast cells. Cell lysates were then harvested and analyzed by immunoprecipitation and Western blot, to identify any differences in PB2-MAVS interactions in avian cells.

Aim 4. Determine the effect of differently adapted PB2 proteins on duck MAVS IFN- β signaling.

The IFN- β inhibitory activities of IAV PB2 proteins on duck MAVS was analyzed *in vitro* by a dual luciferase assay. Duck MAVS, cloned into the expression vector pcDNA3.1/Hygro (Invitrogen), was overexpressed to induce the IFN- β signaling pathway in DF-1 cells. IAV PB2, cloned into the pSMART-CMV expression vector, was co-transfected with duck MAVS. The relative activity of the chicken IFN- β promoter activity was measured and compared between PB2 and non-PB2 treated samples.

Aim 5. Determine the cellular localization of differently adapted IAV PB2 proteins in avian cells.

The cellular localization of PB2 is shown to have an effect on the PB2-mediated inhibition of the IFN response in human cells (8). Differences in PB2 localization with regards to MAVS, could explain variation in PB2-mediated IFN inhibition in avian cells. To identify any differences in PB2 localization in avian cells, PB2 and duck MAVS expression vectors were co-transfected in

DF-1 chicken fibroblast cells. DF-1 cells were then fixed, stained, and analyzed by confocal microscopy.

Aim 6. Determine the significance of PB2 residue 9 in PB2 function.

The D9N mutation in PB2 is characterized as an adaptive mutation that allows IAV strains to infect humans (80). Residue 9 is known to affect the localization of PB2 proteins within human cells (8). To investigate the effects of an avian adaptive (D9) or human adaptive (N9) residue at position 9, mutations that swapped the avian and human adaptive residues were performed in all cloned PB2 proteins. The PB2-MAVS interactions, PB2-mediated IFN- β inhibition, and PB2 localization were all analyzed for the newly generate PB2 mutants as previously described above.

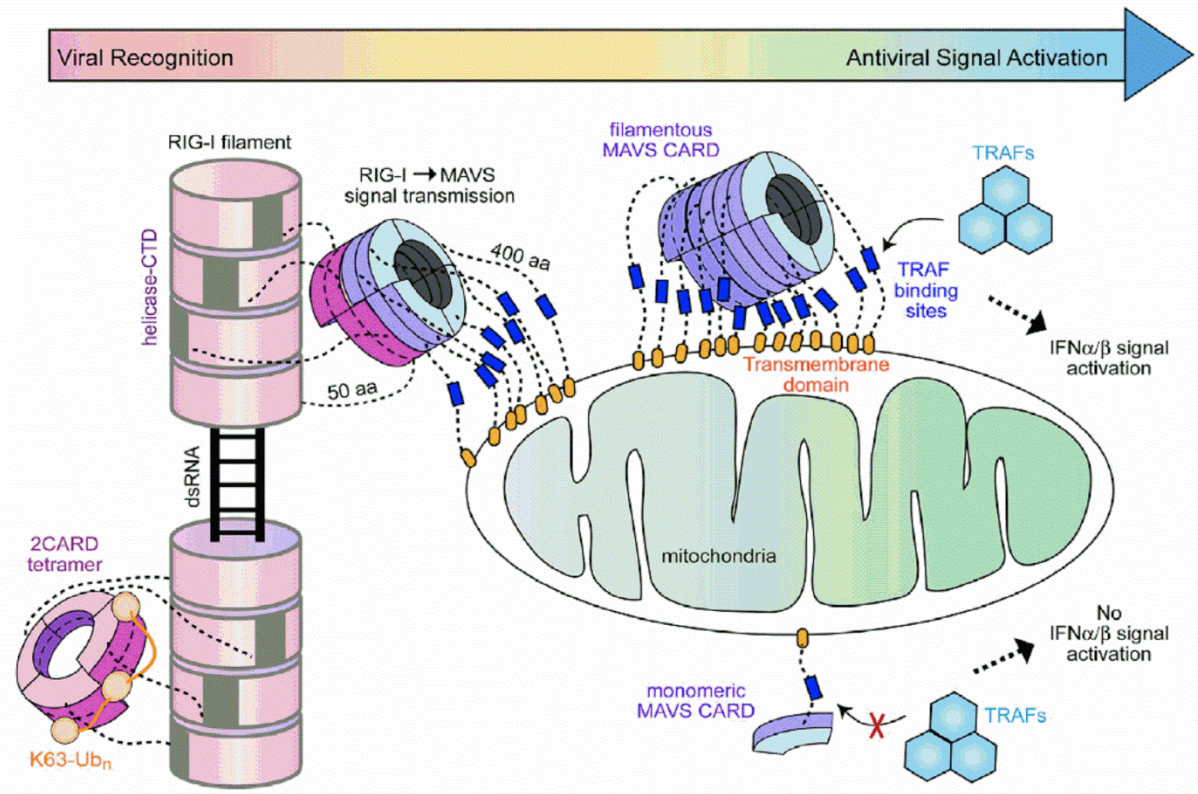


Figure 1. Graphical representation of the RIG-I-MAVS signaling pathway. The helicase and C-terminal domain (CTD) of RIG-I recognizes and binds to viral 5' triphosphate dsRNA and forms filamentous oligomers on the ends of the dsRNA molecule (74). Once bound, the 2CARD^{RIG-I} from four RIG-I proteins are in close enough proximity to induce tetramerization. This interaction is facilitated by a flexible 50 aa linker region between the 2CARD^{RIG-I} and the CTD. Further stabilization of the 2CARD^{RIG-I} tetramer can occur by the addition of K63 linked ubiquitin chains. The resulting tetramer resembles a lock-washer and can now nucleate MAVS filament formation by interacting with multiple MAVS CARDS, via transient interactions. MAVS CARDS are connected to the transmembrane domain of MAVS by a flexible 400 aa long linker region, which contains many TRAF binding sites. TRAFs are important adaptor proteins that activate further downstream proteins to carry out the IFN signal. MAVS CARD filaments bring multiple TRAF binding sites into close proximity and allow for efficient recruitment and activation of TRAFs, which would facilitate the propagation of the antiviral signal to produce Type-I IFN. Note figure is taken from Wu *et al.* (72).

Chapter 2. Materials and Methods

2.1 Viruses

PB2 proteins cloned from 6 different influenza A virus strains were used during this study. I cloned PB2 from two low pathogenic avian influenza (LPAI) strains: A/Dk/British Columbia/500/2005 (BC500) and A/duck/Memphis/546/1974(H11N9) (M546). These LPAI strains were both environmental isolates from infected ducks. PB2 was also cloned from two high pathogenic avian influenza (HPAI) strains: A/Dk/D4AT/71.1/2004 (H5N1) (D4AT) and A/Vietnam/1203/2004 (H5N1) (VN1203). D4AT was isolated from an infected duck, while VN1203 was isolated from a fatal human case. As well, I cloned PB2 from two mammalian influenza strains: A/Puerto Rico/8/1934 (H1N1) (PR8) and A/X-31/2003 (H3N2) (X31). Both PR8 and X31 are mouse adapted lab strains of influenza, which contain several conserved human adaptive residue within the PB2 protein. PR8 was isolated from a human case, while X31 was lab generated.

2.2 Cloning and Plasmids

The Phusion[®] High-Fidelity DNA Polymerase (New England BioLabs) was used in all PCR reactions involved in cloning. The pcDNA3.1/Hygro+ mammalian expression vector (Invitrogen) was used as the backbone to clone and express the constructs containing duck MAVS and duck MAVS-V5. Duck MAVS was initially cloned into the pCR[®]2.1-TOPO (Invitrogen) vector by Ximena Fleming. I then PCR amplified duck MAVS from this previously cloned construct and cloned it into the multiple cloning site (MCS) of the mammalian expression vector pcDNA3.1/Hygro+, using the NheI-BamHI restriction sites encoded within the primers

listed in Table 1. MAVS-V5 was then amplified from the pcDNA-MAVS construct with the addition of an N-terminal V5 epitope tag encoded within the 5' primer. Again, duck MAVS-V5 was cloned into pcDNA3.1/Hygro+ (Invitrogen) using the NheI-BamHI restriction sites. Both duck MAVS constructs were confirmed by sequencing using the primers listed in Table 2. A vector map of pcDNA-MAVS can be found in Figure 2.

To insure that both MAVS constructs were functional in DF-1 cells, 150 ng of duck MAVS and duck MAVS-V5 were transfected into DF-1 cells and the chicken IFN- β promoter activity was assessed via a dual luciferase reporter assay (Figure 3). Briefly, DF-1 cells were seeded (2×10^5 cells/well) in 24 well plates for 24 h, then transfected with a total of 310 ng DNA/well using the Lipofectamine 2000® reagent (Invitrogen) at a ratio of 1 μ g DNA to 2.5 μ L Lipofectamine. The chicken IFN- β promoter luciferase reporter plasmid (pGL3-chIFN β), constructed from the chicken *IFN2* gene was used to assess the relative activity of the chicken IFN- β promoter as previously described (82–84). DF-1 cells were transfected with a constant amount of pGL3-chIFN β (150 ng DNA/well). To serve as an internal control, the *renilla* luciferase reporter construct (phRTK) was co-transfected with pGL3-chIFN β at 10 ng DNA/well. The relative luciferase activity of pGL3-chIFN β compared to phRTK was measured using the Dual-Luciferase Reporter Assay System (Promega) 24 h after transfection. As displayed in Figure 3, both duck MAVS and duck MAVS-V5 constructs are capable of increasing the activity of the chicken IFN- β promoter activity in DF-1 cells. This indicates duck MAVS can function in DF-1 cells.

To clone the 6 different IAV PB2 proteins used in this study, RNA was obtained from infected embryonated chicken egg allantoic fluid using TRIzol (Ambion™), or from previously infected duck tissue RNA samples (82). Viral RNA was then reverse transcribed into cDNA using the SuperScript® III First-Strand Synthesis System (Invitrogen) according to the protocol provided by using 500ng of an influenza specific universal primer (Uni12) (85). PB2 was then amplified in three pieces using overlap extension PCR to avoid problematic mis-priming. Fully amplified PB2 from each strain was then cloned into our pSMART-CMV vector using the KpnI/Nhe1-Not1 cut sites encoded within the primers listed in Table 1. A full vector map of pSMART-CMV-PB2 can be found in Figure 4. pSMART-CMV was constructed by taking the open pSMART-LCKan vector (Lucigen) and ligating in the amplified CMV promoter, MCS, and BGH polyadenylation signal from pcDNA3.1/Hygro+ (Invitrogen) (Figure 5). This was done to counteract the toxic effects PB2 was displaying in our regular copy vectors. D9N and N9D PB2 mutations were performed by amplifying each PB2 with a slightly different 5' primer containing the single nucleotide mutation. PCR amplified mutant PB2 was then cloned into our constructed pSMART-CMV vector using the same Nhe1-Not1 cloning sites. All PB2 constructs were confirmed by sequencing using the primers listed in Table 2. A list of primers used to amplify the pcDNA3.1/Hygro+ (Invitrogen) promoter can be found in Table 3.

2.3 IFN- β reporter assays in collaboration with Sun Hur

Spontaneously immortalized chicken embryonic fibroblasts cells (DF-1), derived from East Lansing strain eggs (86), were maintained in DMEM plus 10% FBS at 39°C and 5% CO₂. Cells were seeded (2×10^5 cells/well) in 24 well plates for 24 h then transfected with a total of 185 ng DNA/well using the Lipofectamine 2000® reagent (Invitrogen) at a ratio of 1 μ g DNA to 2.5 μ L

Lipofectamine. The chicken IFN- β promoter luciferase reporter plasmid (pGL3-chIFN β), constructed from the chicken *IFN2* gene was used to assess the relative activity of the chicken IFN β promoter as previously described (82–84). DF-1 cells were transfected with a constant amount of pGL3-chIFN β (150 ng DNA/well). To serve as an internal control, the *renilla* luciferase reporter construct (phRTK) was co-transfected with pGL3-chIFN β at 10 ng DNA/well. Full length duck MAVS and RIG-I 2CARD (RCC) constructs were transfected at 25 ng DNA/well. The relative luciferase activity of pGL3-chIFN β compared to phRTK was measured using the Dual-Luciferase Reporter Assay System (Promega) 24 h after transfection. The full materials and methods for the Cryo-EM microscopy and HEK 293T cell transfections can be found in the supplemental experimental procedures section in my collaborative work with Sun Hur (72).

2.4 PB2 protein structure modeling and alignment

To create a 3D structure of the IAV PB2 protein, the PB2 amino acid sequence from the PR8 IAV strain was uploaded to the SWISS-MODEL Server (87). SWISS-MODEL then automatically identified and ranked suitable template structures based on Blast (88) and HHblits (89) results from the PDB database (90). The PDB entry 4WSB (91) of the bat Influenza A polymerase was selected to model the PB2 for IAV strain PR8, as it is currently the only full length crystal structure available for the IAV PB2 protein. The resulting PDB file was then exported and analyzed in Pymol (Schrödinger). A sequence alignment of PB2s was generated using T-COFFEE with default settings in Jalview (92). Within the PB2 sequence alignment, the position of known human adaptive residues were indicated (*) (80).

2.5 Immunoprecipitation and Western blotting

Dynabeads (Novex™) coated in protein G were used for the immunoprecipitation experiments. The indirect method as outlined in the Dynabeads (Novex™) protocol was used in this study. Briefly, spontaneously immortalized chicken embryonic fibroblasts cells (DF-1), derived from East Lansing strain eggs (86), were maintained in DMEM plus 10% FBS at 39°C and 5% CO₂. Cells were seeded (8×10^5 cells/well) in 6 well plates for 24 h then transfected with 2 µg DNA of each expression construct using the Lipofectamine 2000® reagent (Invitrogen), at a ratio of 1 µg DNA to 2.5 µL Lipofectamine. 24 h post-transfection, cells were washed in ice cold PBS and lysed for 45 minutes in 250µL/well of Tris Lysis buffer (50mM Tris-HCl, pH 8.0, 200mM NaCl, 25% glycerol, 0.5% Igepal CA-630, 1mM dithiothreitol [DTT], 1 tablet/10 mL of Complete Mini EDTA-free protease inhibitor cocktail [Roche]). 400 µL of clarified cell lysates were incubated with 1 µg rabbit polyclonal PB2 antibody (GeneTex) for 2 h at room temperature. Bound antibody and lysates were then added to 1.2 mg of Dynabeads® protein G and allowed to incubate for 10 minutes at room temperature. Beads were then washed with Tris wash buffer (10 mM Tris-HCl, pH 8.0, 150mM NaCl, 0.1% Igepal CA-630) three times, resuspended in 80 µL of 2x laemmli buffer, and boiled for 10 minutes. For Western blotting, lysates and immunoprecipitated proteins were separated by SDS-PAGE and transferred to a nitrocellulose membrane. Immunoblotting (IB) was performed using either a primary mouse anti-V5 monoclonal antibody at 1:5000 (Invitrogen), or a primary rabbit anti-PB2 polyclonal antibody at 1:5000 (GeneTex), followed by detection with either a secondary goat anti-mouse HRP at 1:5000 (BioRad), or a secondary goat anti-rabbit HRP at 1:5000 (Santa Cruz Biotechnology). Antibodies were then visualized by chemiluminescence using the ECL kit (GE-Healthcare).

2.6 IFN- β reporter assays for PB2 and MAVS

DF-1 cells were seeded (2×10^5 cells/well) in 24 well plates for 24 h, then transfected with a total of 685 ng DNA/well using the Lipofectamine 2000® reagent (Invitrogen) at a ratio of 1 μ g DNA to 2.5 μ L Lipofectamine. The chicken IFN- β promoter luciferase reporter plasmid (pGL3-chIFN β), constructed from the chicken *IFN2* gene was used to assess the relative activity of the chicken IFN- β promoter as previously described (82–84). DF-1 cells were transfected with a constant amount of pGL3-chIFN β (150 ng DNA/well). To serve as an internal control, the *renilla* luciferase reporter construct (phRTK) was co-transfected with pGL3-chIFN β at 10 ng DNA/well. The indicated MAVS and PB2/control constructs were transfected at 25ng/well and 500ng/well respectively. The relative luciferase activity of pGL3-chIFN β compared to phRTK was measured using the Dual-Luciferase Reporter Assay System (Promega) 24 h after transfection.

2.7 Fluorescent microscopy and localization analysis

DF-1 cells were seeded (8×10^5 cells/well) onto glass coverslips in 6 well plates, and transfected with 2 μ g of pcDNA-MAVS-V5 and pSMART-CMV-PB2 constructs. 24 h post-transfection, DF-1 cell mitochondria were labelled with 400 nM of MitoTracker® Red CMXRos (Molecular Probes™) and incubated for 1 h at 39°C. Cells were then fixed overnight in 1% PFA at 4°C. The cellular location of each PB2 protein was determined by staining with a primary rabbit anti-PB2 antibody (GeneTex), followed by secondary detection with a goat anti-rabbit conjugated to Alexa Fluor® 647 (Novex™). Duck MAVS-V5 was stained using a mouse anti-V5 primary monoclonal antibody (Invitrogen), followed by secondary detection with a goat anti-mouse

antibody conjugated to Alexa Fluor[®] 488 (Novex[™]). The nuclei of cells were stained with Hoechst 33342 (Molecular Probes[™]). Eight cells were analyzed for each treatment and images were taken on a Leica TCS SP5 confocal microscope. Image analysis was done using the ImageJ program (93). Localization analysis of duck MAVS and PB2 was done by analyzing the signal intensity values along a defined yellow intensity line through the nucleus and cytoplasm of each analyzed cell. To reduce signal noise, an average intensity value of three pixels was taken for each position along the intensity line. To analyze the percent of non-nuclear PB2 staining, each cell's raw integrated density value for PB2 staining was measured. The difference between total cell PB2 signal and nuclear PB2 signal, was reported as a percentage of total PB2 signal (percent non-nuclear stain). Background noise was removed from each image before analysis by using the Rolling Ball Background Subtraction tool set at 100 pixels within ImageJ.

Table 1. Primer sequences for amplification of duck MAVS and IAV PB2s.

| Gene | Primer | Primer Sequence (5' to 3') |
|-----------------------|---------------|--|
| <i>Duck MAVS</i> | Forward | GCCTGCTAGCATGGGTTTCGCGGAGGACAAGGTG |
| | Reverse | CGGAGGATCCCTACTATTTCTGCAGCCGGGCGTAC |
| | Forward V5 | GCCTGCTAGCATGGGCAAGCCCATCCCCAACCCCTTGCTTGGCTTGGACTC CACCGGTTTCGCGGAGGACAAGGTG |
| <i>PB2 BC500</i> | Forward | GCCTGGTACCATGGAGAGAATAAAAAGAATAAGAGATC |
| | Reverse | ATTCGCGGCCGCCTACTAATTGATGGCCATCCGAAT |
| <i>PB2 M546</i> | Forward | GCCTGGTACCATGGAGAGAATAAAAAGAGCTGAGAGATC |
| | Reverse | ATTCGCGGCCGCCTACTAATTGATGGCCATCCGAAT |
| <i>PB2 D4AT</i> | Forward | GCCTGCTAGCATGGAGAGAATAAAAAGAATTACGAGATC |
| | Reverse | ATTCGCGGCCGCCTACTAATTGATGGCCATCCGAAT |
| <i>PB2 VN1203</i> | Forward | GCCTGCTAGCATGGAGAGAATAAAAAGAATTACGAGATC |
| | Reverse | ATTCGCGGCCGCCTACTAATTGATGGCCATCCGAAT |
| <i>PB2 PR8</i> | Forward | GCCTGGTACCATGGAAAAGAATAAAAAGAATAAGAAATCTA |
| | Reverse | ATTCGCGGCCGCCTACTAATTGATGGCCATCCGAAT |
| <i>PB2 X31</i> | Forward | GCCTGGTACCATGGAAAAGAATAAAAAGAATAAGAAATCTA |
| | Reverse | ATTCGCGGCCGCCTACTAATTGATGGCCATCCGAAT |
| <i>PB2 BC500 D9N</i> | Forward | GCCTGCTAGCATGGAAAAGAATAAAAAGAATAAGAAATCTA |
| | Reverse | ATTCGCGGCCGCCTACTAATTGATGGCCATCCGAAT |
| <i>PB2 M546 D9N</i> | Forward | GCCTGCTAGCATGGAAAAGAATAAAAAGAATAAGAAATCTA |
| | Reverse | ATTCGCGGCCGCCTACTAATTGATGGCCATCCGAAT |
| <i>PB2 D4AT D9N</i> | Forward | GCCTGCTAGCATGGAAAAGAATAAAAAGAATAAGAAATCTA |
| | Reverse | ATTCGCGGCCGCCTACTAATTGATGGCCATCCGAAT |
| <i>PB2 VN1203 D9N</i> | Forward | GCCTGCTAGCATGGAAAAGAATAAAAAGAATAAGAAATCTA |
| | Reverse | ATTCGCGGCCGCCTACTAATTGATGGCCATCCGAAT |
| <i>PB2 PR8 N9D</i> | Forward | GCCTGCTAGCATGGAGAGAATAAAAAGAATAAGAGATC |
| | Reverse | ATTCGCGGCCGCCTACTAATTGATGGCCATCCGAAT |
| <i>PB2 X31 N9D</i> | Forward | GCCTGCTAGCATGGAGAGAATAAAAAGAATAAGAGATC |
| | Reverse | ATTCGCGGCCGCCTACTAATTGATGGCCATCCGAAT |

Table 2. Primer sequences for sequencing of duck MAVS and IAV PB2s.

| Gene | Primer | Primer Sequence (5' to 3') |
|-----------------------------|---------------|-----------------------------------|
| <i>Duck MAVS</i> | T7-pgem | TAATACGACTCACTATAGGG |
| | Forward | ATGGGTTTCGCGGAGGACAAG |
| | Reverse | CTATTTCTGCAGCCGGGCGTAC |
| | BGHR | TAGAAGGCACAGTCGAGG |
| <i>PB2 (excluding HPAs)</i> | SR2 | GGTCAGGTATGATTTAAATGGTCAGT |
| | T7-pgem | GTAATACGACTCACTATAGGG |
| | F2 | TTCCTCCCAGTGGCTGGT |
| | F3 | GTGGCCATGGTATTTTCAACAAGA |
| | SL1 | CAGTCCAGTTACGCTGGAGTC |
| <i>PB2 HPAs</i> | SR2 | GGTCAGGTATGATTTAAATGGTCAGT |
| | T7-pgem | GTAATACGACTCACTATAGGG |
| | F2 | TGTTGGAAAGGGAAGTGGT |
| | F3 | GTAGCAATGGTGTTCACAGGA |
| | SL1 | CAGTCCAGTTACGCTGGAGTC |

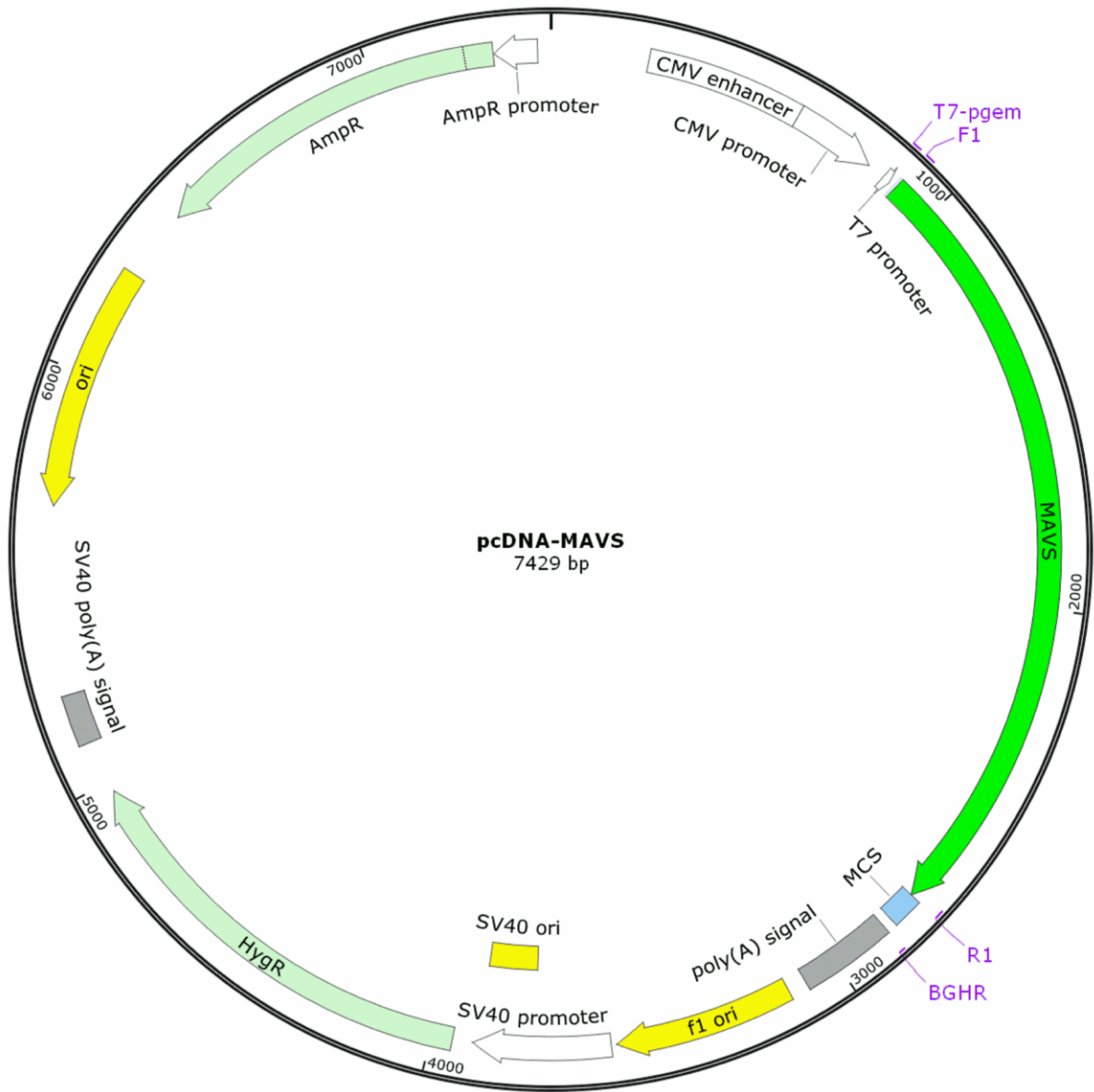


Figure 2. Vector map of pcDNA3.1/Hygro+ with a duck MAVS insert. MAVS was directionally cloned into the pcDNA3.1 vector using NheI and BamHI restriction cut sites. Location of sequencing primers are indicated and labelled in purple. Image was generated in SnapGene®.

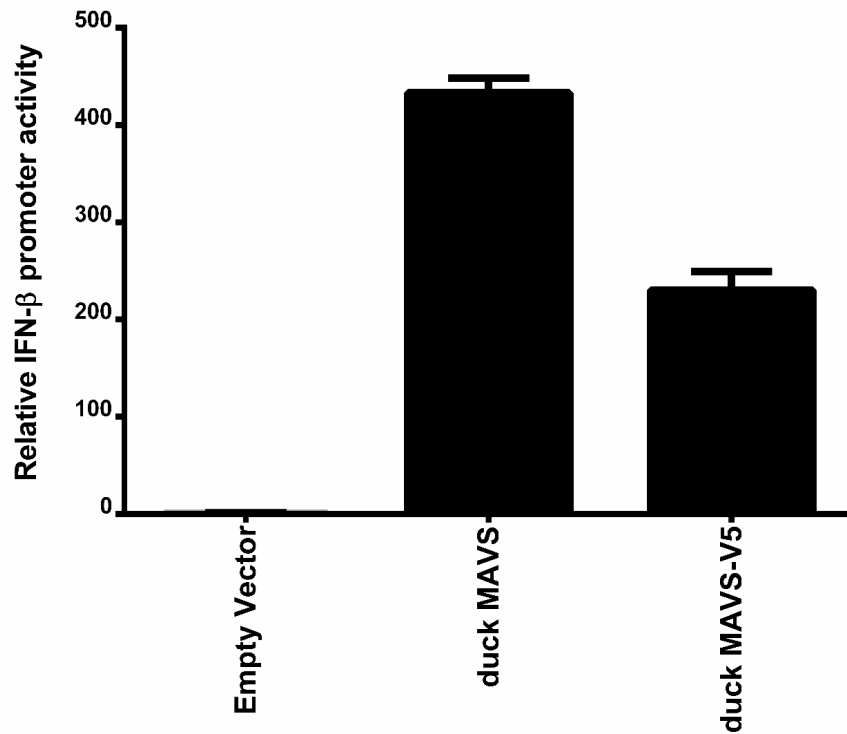


Figure 3. The effect of duck MAVS and duck MAVS-V5 on the chicken IFN- β promoter activity. DF-1 cells were co-transfected with either pcDNA-dMAVS (150ng) or pcDNA-dMAVS-V5 (150ng). The relative luciferase activity of pGL3-chIFN β compared to phRTK (*renilla* luciferase) was measured using the Dual-Luciferase Reporter Assay System (Promega) 24 h after transfection. Mean values were calculated from the average of 3 measurements obtained from 1 independent experiments (n=1). Error bars represent the standard deviation from the means.

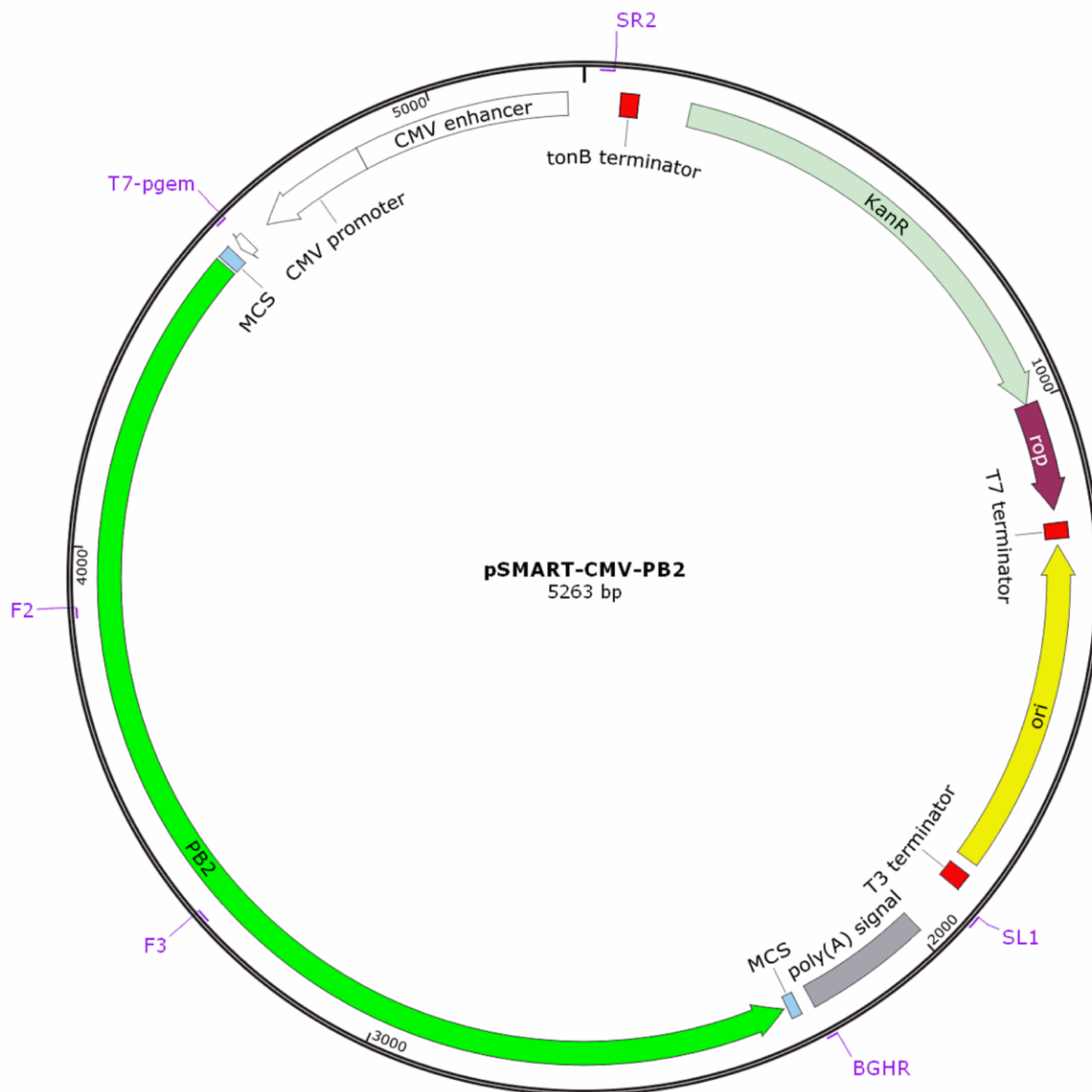


Figure 4. Vector map of pSMART-CMV with an influenza A PB2 insert. PB2s were directionally cloned into a constructed pSMART-CMV vector using NheI/KpnI and NotI restriction cut sites. Location of sequencing primers are indicated and labelled in purple. Image was generated in SnapGene®.

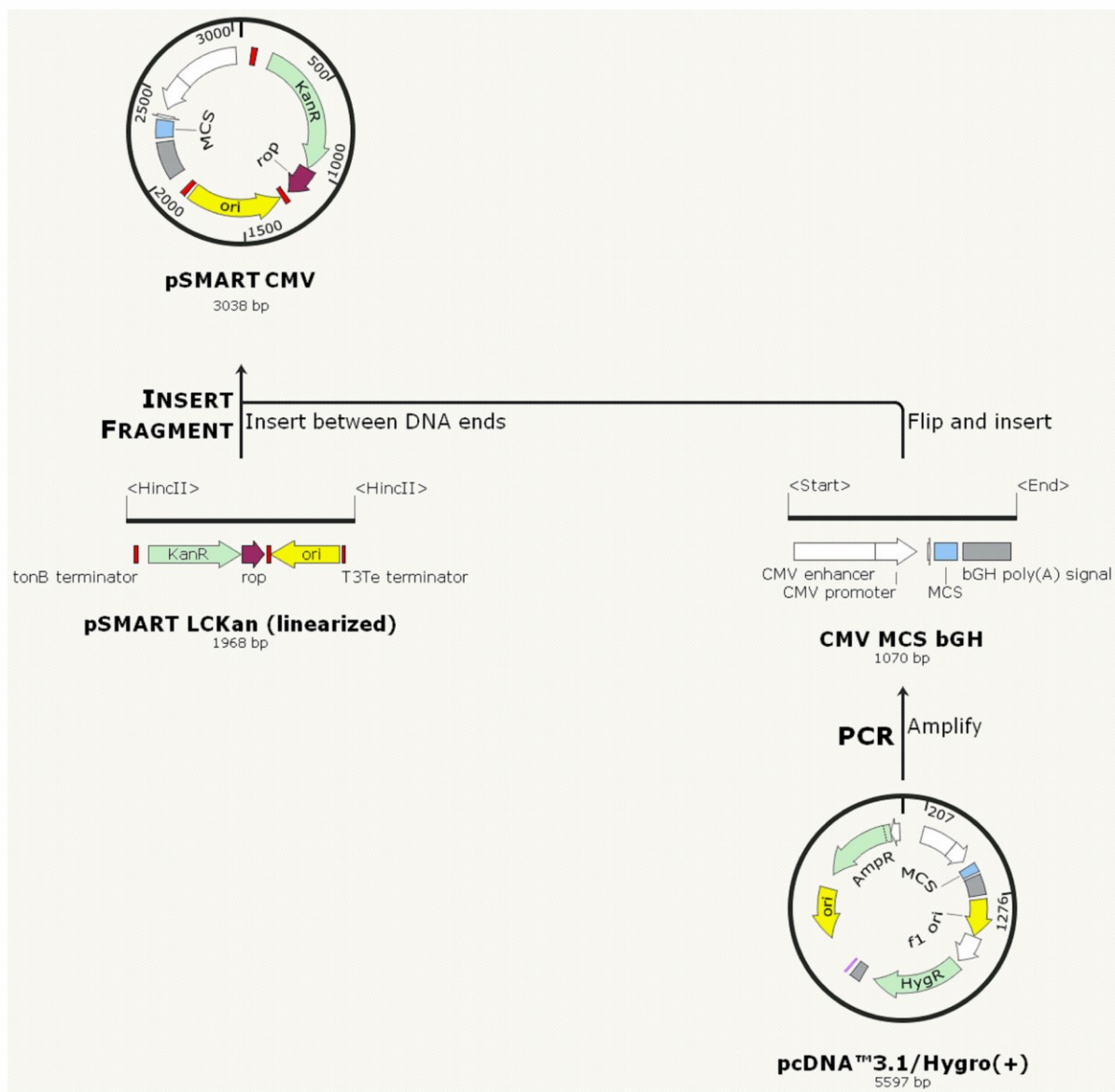


Figure 5. Flow chart depicting the method in which the pSMART-CMV expression vector was generated. The CMV promoter, multiple cloning site, and polyadenylation signal was amplified using the primers in Table 3. The amplified pcDNA fragment then flipped and inserted in the already linearized pSMART LCKan vector (Lucigen), creating the expression plasmid pSMART-CMV. Flow chart was generated using SnapGene®.

Table 3. Primer sequences for amplification of the CMV promoter from pcDNA3.1/Hygro+.

| Vector | Primer | Primer Sequence (5' to 3') |
|----------|--------------|----------------------------|
| pcDNA3.1 | 5' of CMV F | TAATACGACTCACTATAGGG |
| | 3' of BGHR R | TAGAAGGCACAGTCGAGG |

Chapter 3. Results

3.1 A T175/T176 mutation in duck 2CARD^{RIG-I} enables IFN signaling in human cells.

Duck RIG-I cannot activate the MAVS-mediated IFN signaling pathway in human cells. Similarly, human RIG-I cannot activate the MAVS-mediated IFN signaling pathway in avian cells (94). This observation is thought to be caused by variances in the 2CARD of RIG-I between humans and ducks (Figure 6A), as exogenous RIG-I proteins cannot interact with endogenous MAVS to initiate the IFN signal. However, upon superimposing the duck 2CARD^{RIG-I} onto the human 2CARD^{RIG-I} structure, it was identified by Sun Hur, that only two loops in the IIB/IIA 2CARD^{RIG-I}:CARD^{MAVS} interface significantly deviated between the human and duck RIG-I proteins (Figure 6B and C). Therefore, in an effort to restore duck MAVS signaling in human cells and test a model of RIG-I-MAVS activation, the corresponding duck 2CARD^{RIG-I} residues were mutated to the equivalent human residues (E115TR and T175K/T176E). We found that an E115TR mutation/insertion in duck 2CARD^{RIG-I} abrogated the IFN- β promoter activity in ducks and did not improve the IFN signaling in HEK293T cells (Figure 6D and E). However, a T175K/T176E mutation in duck 2CARD^{RIG-I} increased the IFN- β promoter activity to within 70% of the human 2CARD^{RIG-I} activity in HEK293T cells (Figure 6E). Interestingly, the T175K/T176E mutation in duck 2CARD^{RIG-I} did not significantly inhibit the IFN- β promoter activity in chicken DF-1 cells (Figure 6D). This could suggest plasticity in the 2CARD^{RIG-I}:CARD^{MAVS} interaction, considering how different the 2CARD^{RIG-I} interface is between humans and ducks.

3.2 Mutations at residues 43 and 56 in both duck and human MAVS abrogates MAVS-mediated IFN signaling.

A recent publication (95) presented a competing model of MAVS filament formation, that was different from the one proposed by Sun Hur (72). To aid in identifying which model was correct, mutations were introduced at specific residues that differed in position between the two models. MAVS residues 43 and 56 were prime candidates, as both residues fell within the Ia/Ib $CARD^{MAVS}:CARD^{MAVS}$ interface of the MAVS filament, and were shown to be in close proximity to each other in only one of the competing models (Figure 7A, B, and E). A mutation at either one of these positions should inhibit the MAVS-mediated IFN signalling if these residue interactions are important for the MAVS filament, which they are predicted to be by the Sun Hur (72) model but not the Xu *et al.* (95) model. We found that IFN- β promoter activity was abrogated upon mutation of either residue 43 or 56 in both human (Figure 7C) and duck (Figure 7D) MAVS. In an effort to restore signaling and reaffirm an interaction between these residues, a charge complimentary mutation in both human (W56R and R43D/E) and duck (Y56R and H43D/E) MAVS was performed. Although deformed and irregular MAVS filaments were detected in the charge complimentary double mutants (Figure 7F), IFN- β signaling could only be partially restored in human MAVS but not duck MAVS. Together, these results suggest there is a direct interaction between MAVS residues 43 and 56 in both duck and human MAVS that aid in MAVS filament formation, suggesting that the Sun Hur model (72) correctly predicts the mechanism of MAVS filament formation.

3.3 Modeling influenza PB2 illustrates three human adaptive residues near the PB2 MAVS binding domain.

Previously, PB2 was characterized to contain several adaptive residues that helped determine transmissibility between avian and human hosts (80). These residues had yet to be mapped on a complete crystal structure of an influenza A PB2 protein. To aid in understanding the function of these adaptive residues, I modeled the PB2 (PR8) amino acid sequence to the recently published bat influenza A PB2 crystal structure (4WSB) (91) (Figure 8A). Three adaptive residues were visualized to accumulate within the same domain (N9, T64, M81), though only 1 of these residues (N9) fell within the PB2 domain described to bind human MAVS (79) (Figure 8B and C). Residues N9, T64, and M81 of PB2 (PR8) are located too far apart for any significant intermolecular interactions to occur; however, the residues were found to share a common interface surface, which resembles a potential binding cleft that could bind a conserved secondary structure, such as an α -helix (Figure 8B). An alignment of the 6 PB2 proteins used in this study demonstrates the high sequence conservation of PB2 (> 98% identity), while also highlighting where major differences arise between various IAV strains (Figure 8C). I have identified that PB2 proteins from LPAI, HPAI, and mammalian adapted influenza all differ at the adaptive residues 9, 64, and 81, suggesting that these residues may be important for determining PB2 function. Specifically, I am interested in residue 9 as it is positioned within the characterized PB2 MAVS binding domain (Figure 8C).

3.4 Not all avian influenza PB2 can bind to duck MAVS.

Previously, both mammalian (N9) and avian adapted (D9) PB2 proteins have been shown to bind to human MAVS despite differences at the 9th residue (79). However, duck MAVS shares only ~25% identity with human MAVS and could preferentially interact with avian PB2 over mammalian adapted PB2, due to prolonged coevolution between avian viruses and their hosts. Therefore, to investigate the impact a different MAVS target has on PB2-MAVS interactions, I co-transfected PB2 and duck MAVS in DF-1 cells and analyzed their interaction by immunoprecipitation (IP) and Western blot. As expected, human PB2 from PR8 and X31 IAV strains could interact with duck MAVS (Figure 9A). However, it was unexpected to observe the interaction between duck MAVS and PB2 from LPAIs (BC500 and M546) was weak or not detectable, respectively (Figure 9A). In contrast, the sampled HPAI PB2 proteins (D4AT and VN1203) could elicit a detectable interaction with duck MAVS. Thus, it appears LPAI PB2 proteins display a reduced capability to interact with duck MAVS, while HPAI and mammalian adapted PB2 proteins have acquired this MAVS binding ability.

3.5 The PB2 mutation D9N in the LPAI M546 strain restores duck MAVS binding.

The adaptive PB2 residue at position 9 has produced differences in PB2 localization and IFN- β inhibition in human cells between avian and mammalian adapted IAVs (8). However, it has also been shown to not dramatically impact the MAVS binding capabilities of PB2 (79). To investigate if a 9th residue mutation in PB2 could affect binding to duck MAVS, I performed the IP and Western blot described above with PB2 proteins mutated at the 9th residue, which

swapped avian and mammalian adapted PB2 residues at position 9 (Figure 9B). Interestingly, the PB2 mutation (D9N) in the LPAI M546 restores binding to duck MAVS, while all other PB2-MAVS interactions appear to not be significantly affected by the mutation (Figure 9B). This suggests the 9th residue in PB2 is important for MAVS binding, but it is not the only factor that determines PB2-MAVS binding interactions.

3.6 Mammalian IAV PB2 proteins are potent inhibitors of duck MAVS IFN- β signaling.

PB2 from different IAV strains have been shown to inhibit IFN- β signaling to differing degrees based on the IAV strain and the residue at position 9 of PB2 (8, 9). I speculated this observation was due to specific PB2 mutations incurred by the virus to facilitate a better interaction with the host MAVS. To test this idea, I co-transfected several different IAV PB2 proteins with duck MAVS in DF-1 cells and measured the IFN- β promoter activity. Unexpectedly, mammalian PB2 (PR8, X31) inhibits duck MAVS IFN- β signaling by a greater extent (> 65.4% inhibition) than the avian adapted IAV PB2 proteins (< 48.1% inhibition) (Figure 10). Even upon mutating the 9th residue of PB2 to swap the avian and mammalian adapted residues, mammalian adapted PB2 proteins remain more potent inhibitors of IFN- β signaling (> 46.2% inhibition) than avian PB2 D9N mutants (< 31.9% inhibition) (Figure 10). In fact, after mutating the 9th residue in PB2 a general decrease was seen in IFN- β promoter inhibition, except for the D9N PB2 from the M546 IAV strain, which increases IFN- β inhibition (+17.4%) (Figure 10). This suggests a PB2-MAVS binding interaction contributes to the PB2 inhibition of the MAVS-mediated IFN- β signaling.

3.7 Mammalian adapted PB2 shows partial localization with duck MAVS in avian cells.

The localization of PB2 to the mitochondria is believed to be mediated by the binding of the first 37 N-terminal residues of PB2 to MAVS (79), however it has been speculated that other N-terminal residues could be involved (8, 9). Residue 9 of PB2 is important in determining the cellular localization of PB2. Specifically, mammalian adapted PB2 (N9) is known to localize to the mitochondria, while avian adapted PB2 (D9) does not (8). I speculate that this was due to specific adaptive mutations in mammalian PB2 that allowed for the binding of human MAVS, while avian PB2 would be better adapted to interact with avian MAVS. To test this hypothesis in avian cells, I co-transfected different IAV PB2 proteins with duck MAVS and observed the localization signal of each protein via fluorescent microscopy.

Since a large portion of PB2 proteins localize to the nucleus via a conserved bipartite nuclear localization signal (NLS)(60), only a small amount of the PB2 signal actually localizes with MAVS. Therefore a quantitative co-localization analysis was difficult to perform. Consequently, I decided to observe the signal intensity patterns of PB2 and duck MAVS in relation to one another. This allowed me to begin to annotate differences in the localization patterns of differentially adapted PB2 proteins. To perform this, I analyzed the localization patterns of 8 cells for each transfected PB2 protein. Upon selecting a Z stack that clearly displayed the most amount of MAVS signal in focus, I drew a signal intensity line to cover as much MAVS signal as possible, while still passing the signal intensity line through the nucleus for a point of reference. I was then able to observe the signal intensity of labelled PB2 and MAVS proteins along the intensity line to see if their signals displayed similar patterns, if so, we can begin to infer that their signals are starting to localize to similar positions within the transfected cells.

Upon observation, the avian IAV PB2 proteins (BC500, M546, D4AT, VN1203) demonstrate no significant ability to localize with duck MAVS. The avian adapted PB2 signal is very low and does not synchronize with the signal intensity peaks of duck MAVS (Figure 11). However, mammalian PB2 proteins (PR8, X31) demonstrate a significantly different localization signal pattern. Mammalian adapted PB2 proteins display an increase in signal intensity that begins to synchronize with the duck MAVS signal intensity peaks (Figure 11), which suggests an increase in MAVS localization is occurring for mammalian adapted IAV PB2 proteins. Furthermore, mammalian IAV PB2 (X31) was also shown to localize to the mitochondria when duck MAVS was not transfected, suggesting PB2 does not require activated MAVS to localize to the mitochondria (Figure 12). This is in agreement with what has been observed in Vero cells, where mammalian but not avian adapted IAV PB2 proteins have been characterized as mitochondrial (8). Together these results suggest that mammalian adapted IAV PB2 proteins have acquired an ability to partially localize with MAVS proteins.

3.8 A PB2 mutation at residue 9 causes increased cytoplasmic staining of HPAI and mammalian adapted PB2 proteins.

Previously, residue 9 has been shown to influence the localization of IAV PB2 proteins (8). Therefore, it is suspected that mutating residue 9 of PB2, to swap the avian and mammalian adaptive residues, should dramatically change the localization patterns of these PB2 proteins. To investigate this, I again used fluorescent microscopy to document the location of my mutant PB2 proteins (Mut PB2) and duck MAVS within DF-1 cells (Figure 11). Upon observing the mutant

PB2 images there appears to be negligible change for the BC500 PB2 signal pattern, however an increase in the PB2 signal outside of the nucleus is visible for the M546 D9N PB2 (Figure 11). The D4AT and VN1203 D9N PB2 signals were not shown to localize with duck MAVS (Figure 11). Instead, it appears there is considerably more signal intensity outside of the nucleus, indicating an increase in cytoplasmic localization for the HPAI mutant PB2 proteins. This suggests an asparagine at position 9 is not enough to direct avian PB2 to partially localize with duck MAVS. Similarly the signal of the mutant mammalian PB2 proteins (PR8, X31) appears to no longer associate with duck MAVS signal intensity peaks. Instead, mammalian PB2 demonstrates the same erratic cytoplasmic signal, indicating a decrease in PB2 association with MAVS and an increase in non-targeted cytoplasmic staining (Figure 11). Together, these results suggest residue 9 of PB2 indeed influences PB2 localization within avian cells, however it is not the sole factor involved in PB2 localization to duck MAVS.

3.9 Mammalian adapted IAV PB2 proteins have increased non-nuclear staining that is not dependent on residue 9.

Since differences in PB2 cytoplasmic staining has been observed in Figure 11, I decided to obtain a quantifiable parameter to measure the amount of PB2 staining within the cytoplasm. Each analyzed cell from Figure 11 was also measured for the amount of non-nuclear PB2 staining (Figure 13). This provided another piece of data to help me understand how the PB2 protein was distributed in each transfected cell and how the distribution was affected by a mutation at the adaptive 9th residue of PB2. In agreement with previous results, the wild type mammalian PB2 proteins (PR8, X31) had a higher amount of non-nuclear staining (> 18.7%)

than the wild type avian PB2 proteins (< 7.8%) (Figure 13). However, the PB2 non-nuclear staining of mammalian IAV PB2 proteins was not significantly changed upon an N9D mutation, which has been reported to be responsible for mitochondrial localization of PB2 (8). Furthermore, it appears a mutation of the avian adapted D9 residue, to the mammalian adapted N9 residue impacts avian PB2 proteins differently depending on whether a LPAI or HPAI PB2 is mutated. LPAI PB2 did not display the same increase in non-nuclear staining (< 4.5% increase) as with what is seen in the HPAI PB2 proteins (> 11.0% increase) (Figure 13). These observations along with the localization data suggests mammalian PB2 is unambiguously localized outside of the nucleus to possibly interact with duck MAVS, however the 9th residue is not the sole determinant of cytoplasmic or MAVS associated PB2 localization.

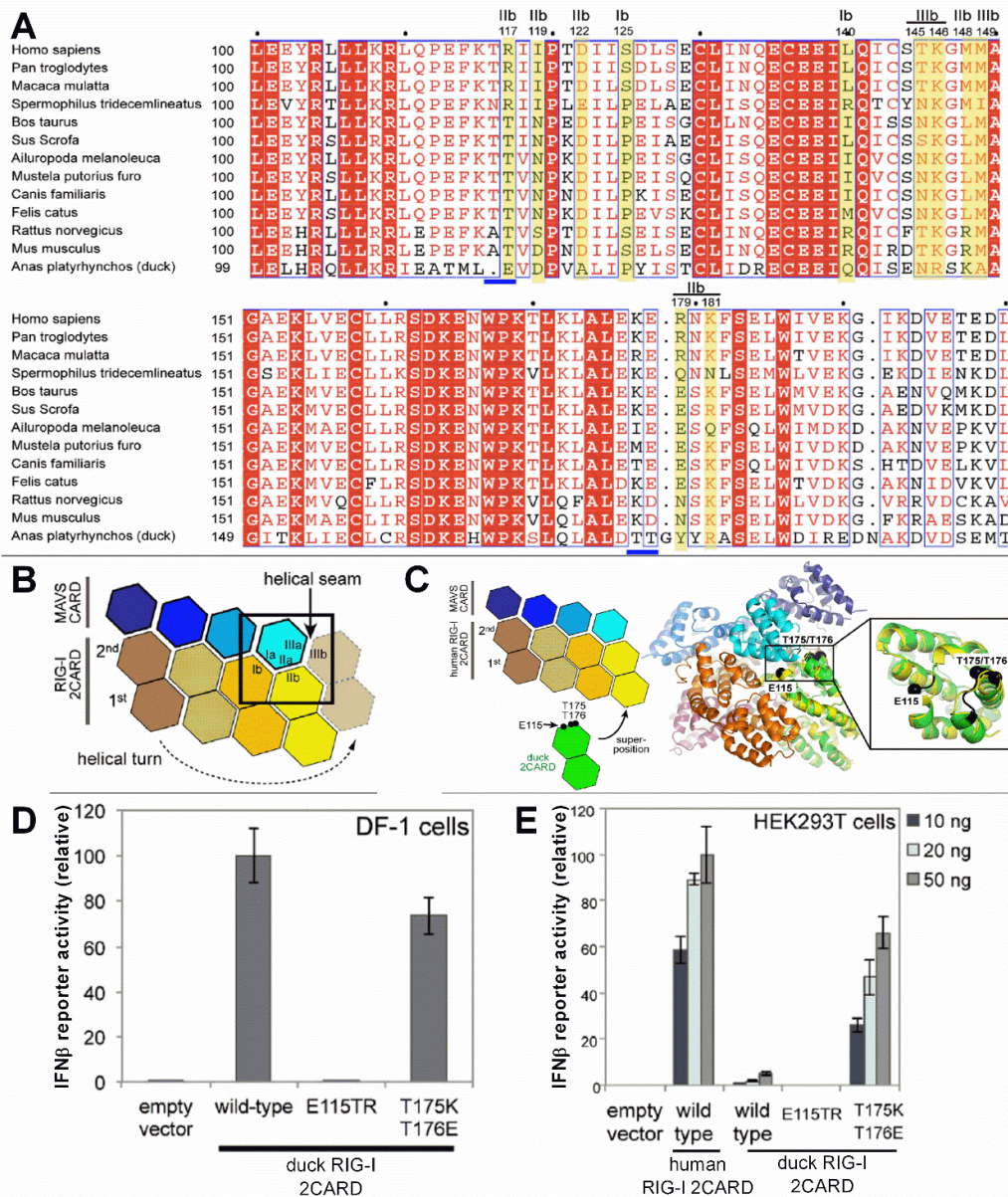


Figure 6. Analysis of the 2CARD^{RIG-I}:CARD^{MAVS} interface. (A) Sequence alignment of the second RIG-I CARD domain between various RIG-I orthologs using the Clustal Omega program. Yellow represents the interface residues and a blue bar represents the residues mutated in duck RIG-I. (B) Graphical mapping of the 2CARD^{RIG-I}:CARD^{MAVS} interfaces. (C) Superposition and graphical representation of duck 2CARD^{RIG-I} (green, PDB 4A2W) onto human 2CARD^{RIG-I} in the 2CARD^{RIG-I}:CARD^{MAVS} complex. Duck residues E115 and T175/T176 are represented by black spheres on the interface surface. (D) Dual luciferase assay of the IFN- β promoter activity in DF-1(D) and HEK293T (E) cells after transfection with varying amounts of wild type or mutant human and duck 2CARD^{RIG-I} domains. Note, all figures taken from Wu *et al.* (72).

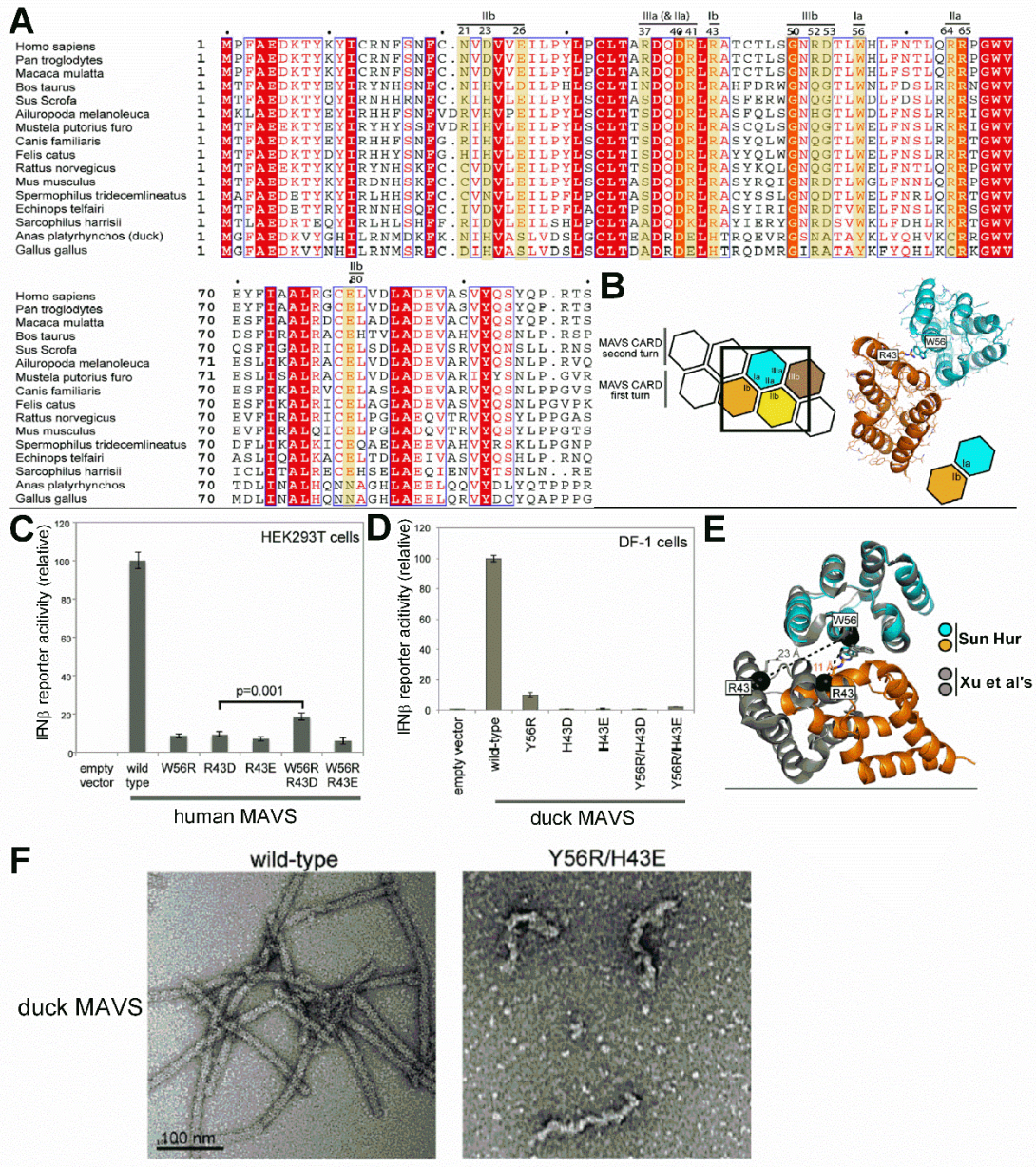


Figure 7. Analysis of the CARD interface within the MAVS filament. (A) Sequence alignment using Clustal Omega of CARD^{MAVS} from various MAVS orthologs. Interface residues are highlighted in yellow. (B) Model of the Ib-Ia CARD^{MAVS} interface within the MAVS filament. Orange and blue colours represent separate CARD^{MAVS} molecules. Residues 43 and 56 are found within the Ib-Ia interface. (C) IFN- β promoter activities during transfection with human MAVS constructs in HEK293T cells. (D) IFN- β promoter activities after transfection with duck MAVS constructs in DF-1 cells. (E) Comparison of the CARD^{MAVS} Ia-Ib interface between the Sun Hur (72) MAVS filament model (orange, cyan) and the competing Xu *et al.* (95) model. (F) Cryo-EM microscopy images of wild type and mutant duck CARD^{MAVS}-S filaments. Note, all figures taken from Wu *et al.* (72).

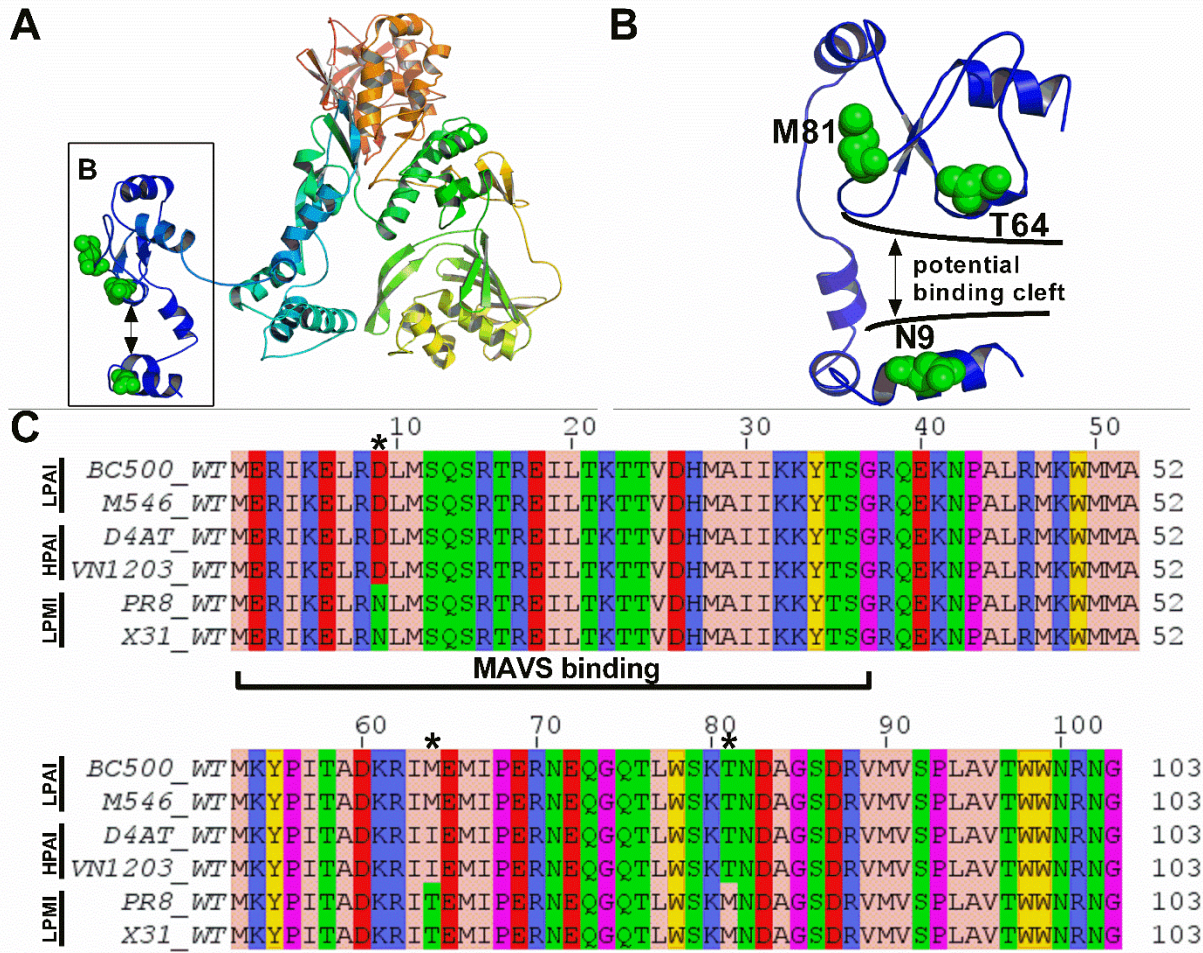


Figure 8. Map of adaptive residues within the PB2 structure. Influenza PB2 exhibits three adaptive residues near the MAVS-PB2 interface. (A) Modeled influenza PB2 (PR8) is shown from the N-terminus (blue) to the C-terminus (red). PB2 (PR8) was modeled to the bat influenza A PB2 crystal structure (4WSB) template using the SWISS-MODEL protein structure homology-modelling server. (B) The first 103 residues of PB2 (PR8) are displayed with the proposed location of the potential MAVS α -helix binding cleft. Highlighted are the locations of three adaptive residues (green) between mammalian and avian influenza strains. (C) An influenza PB2 alignment of the first 103 residues from 6 different influenza strains, 2 low pathogenic avian influenza strains (LPAI), 2 high pathogenic avian influenza (HPAI) strains, and 2 mammalian adapted IAV strains. The residues are coloured according to their physicochemical properties based on the Zappo colour scheme in Jalview. Highlighted are the primary PB2 residues responsible for MAVS binding, as well as the adaptive PB2 residues involved in host adaptation (*).

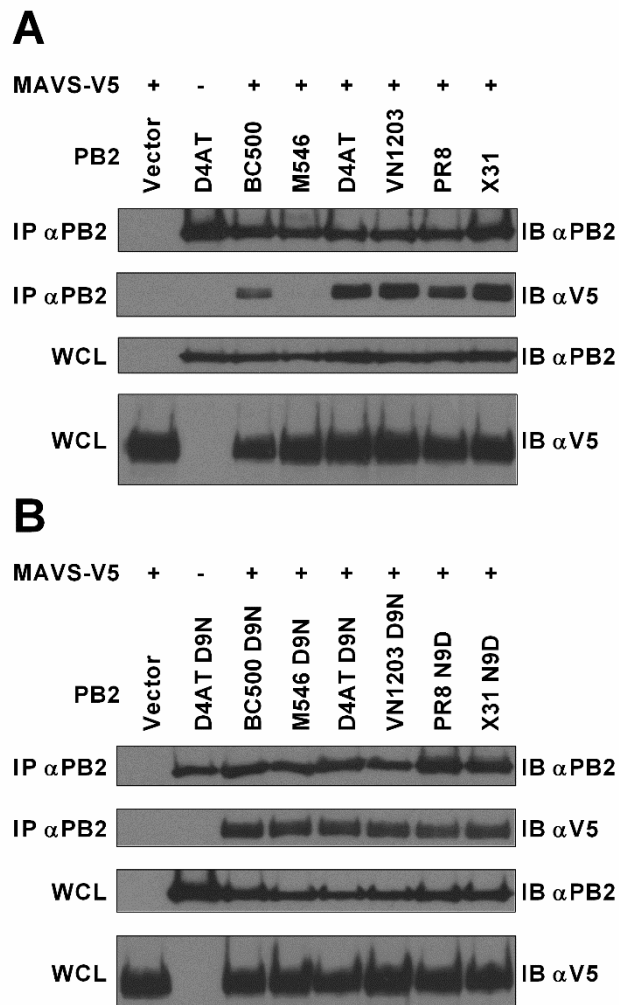


Figure 9. Analysis of PB2-MAVS protein interactions. Avian PB2 (M546) displays no interactions with duck MAVS, while a D9N mutation to the M546 PB2 restores PB2-MAVS interaction. (A) Lysates from DF-1 cells co-transfected with pcDNA-dMAVS-V5 and pSMART-CMV-PB2 from various strains were analyzed by IP using a polyclonal anti-PB2 antibody. MAVS-V5 and PB2 were detected by Western blot for both the IP and whole cell lysate (WCL) samples. (B) Lysates from DF-1 cells co-transfected with pcDNA-dMAVS-V5 and pSMART-CMV-PB2 mutants at the 9th residues were analyzed by co-IP using a polyclonal anti-PB2 antibody. MAVS-V5 and PB2 were detected by Western blot for both the IP and WCL samples. Note immunoprecipitations and Western blots were repeated twice with two independent sets of cell lysate samples.

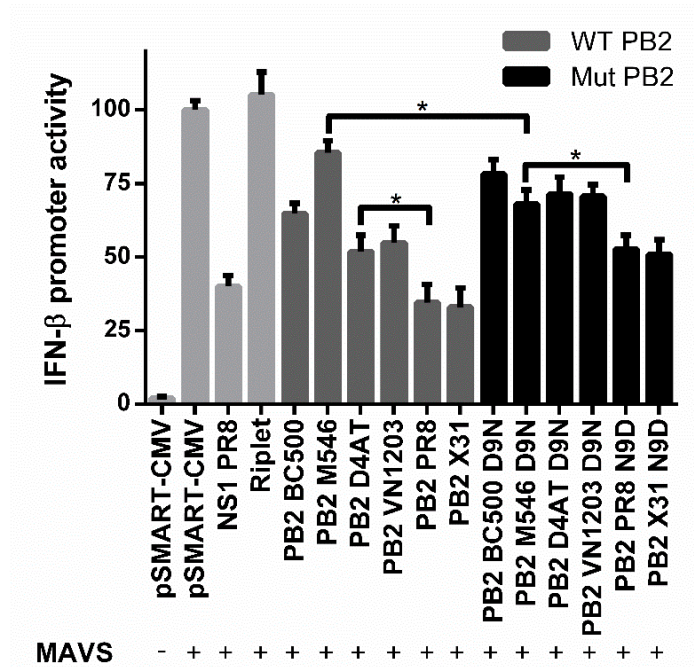


Figure 10. PB2 inhibition of MAVS-mediated IFN signaling. Wild type and mutated mammalian influenza PB2 proteins remain potent inhibitors of chicken IFN- β promoter activity when compared to avian influenza PB2 proteins. DF-1 cells were co-transfected with pcDNA-dMAVS (25ng) and pSMART-CMV-PB2 (500ng) from different influenza strains. The relative luciferase activity of pGL3-chIFN β compared to phRTK (*renilla* luciferase) was measured using the Dual-Luciferase Reporter Assay System (Promega) 24 h after transfection. IAV PR8 NS1 and duck Riplet were used as positive and negative controls. Dark grey bars represent the activity of wild type PB2 proteins, while black bars indicate the activity of mutated PB2 proteins. Mean values were calculated from the average of 9 measurements obtained from 3 independent experiments (n=3). Error bars represent the standard deviation from the means. A one-way ANOVA was conducted to compare effect of PB2 on MAVS-mediated IFN signaling. PB2 displayed a significant effect on the chicken IFN promoter activity ($F[15,32] = 83.28$, $p < 0.0001$). * indicates a P value < 0.05 , based on a Tukey multiple comparison test.

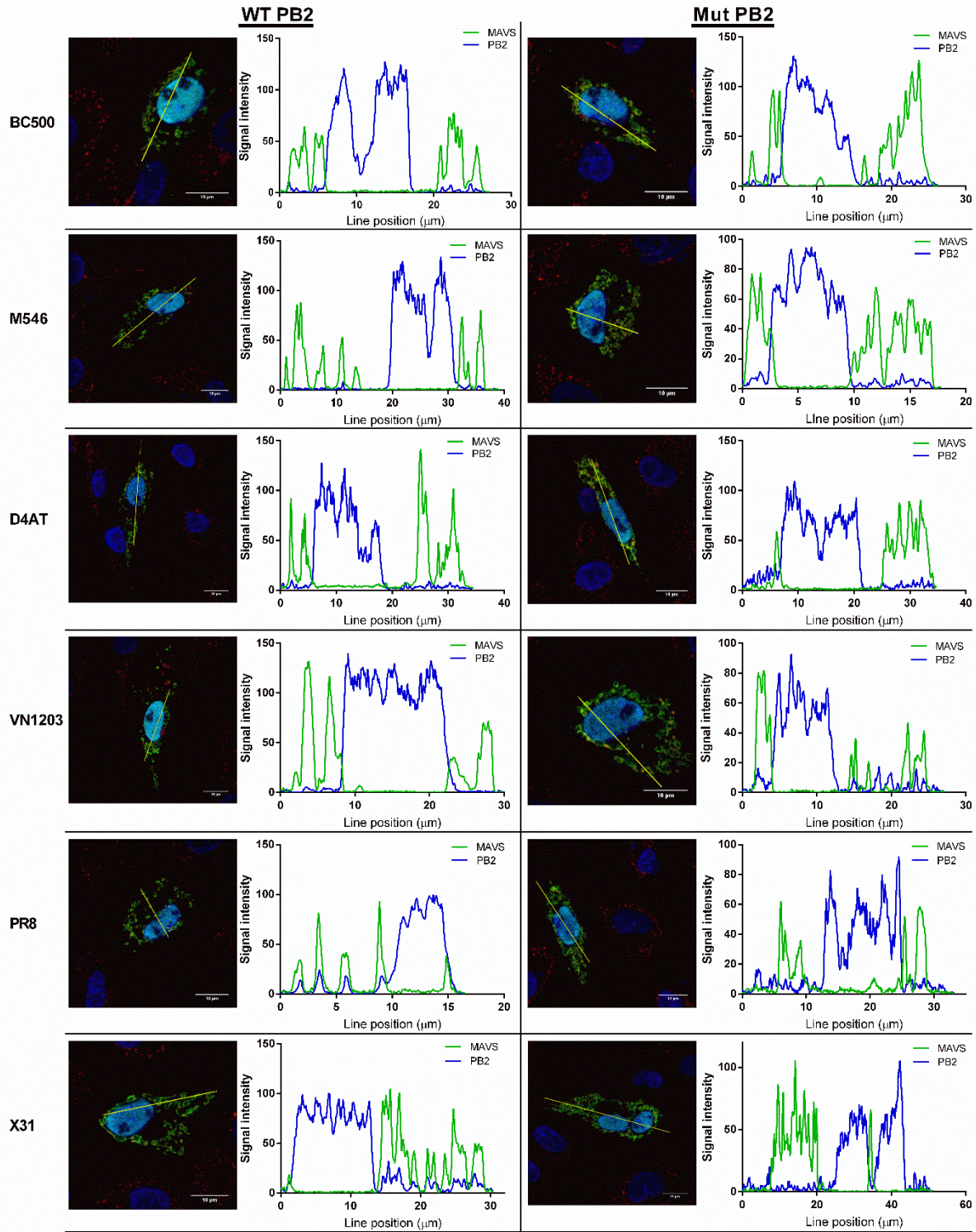


Figure 11. Localization of PB2 and MAVS within DF-1 cells. Mammalian PB2 displays a partial increase in cellular localization to duck MAVS as compared to avian adapted PB2. A N9D mutation of mammalian adapted PB2 disrupts the partial MAVS localization, while a D9N mutation of avian PB2 does not restore the partial PB2 localization with duck MAVS. Confocal images and signal intensity plots are shown depicting the cellular localization of duck MAVS-V5 (green) and wild type or mutant influenza PB2 proteins (blue) within DF-1 cells. Each cellular image is a representative picture from 8 analyzed cells. A yellow line has been drawn in each image to indicate the location of the signal intensity plot. An average of three pixels was used to generate the signal intensity plot after background noise was subtracted from all images using the Rolling Ball Background Subtraction tool within ImageJ. The scale bar represents a 10 μm length within each image.

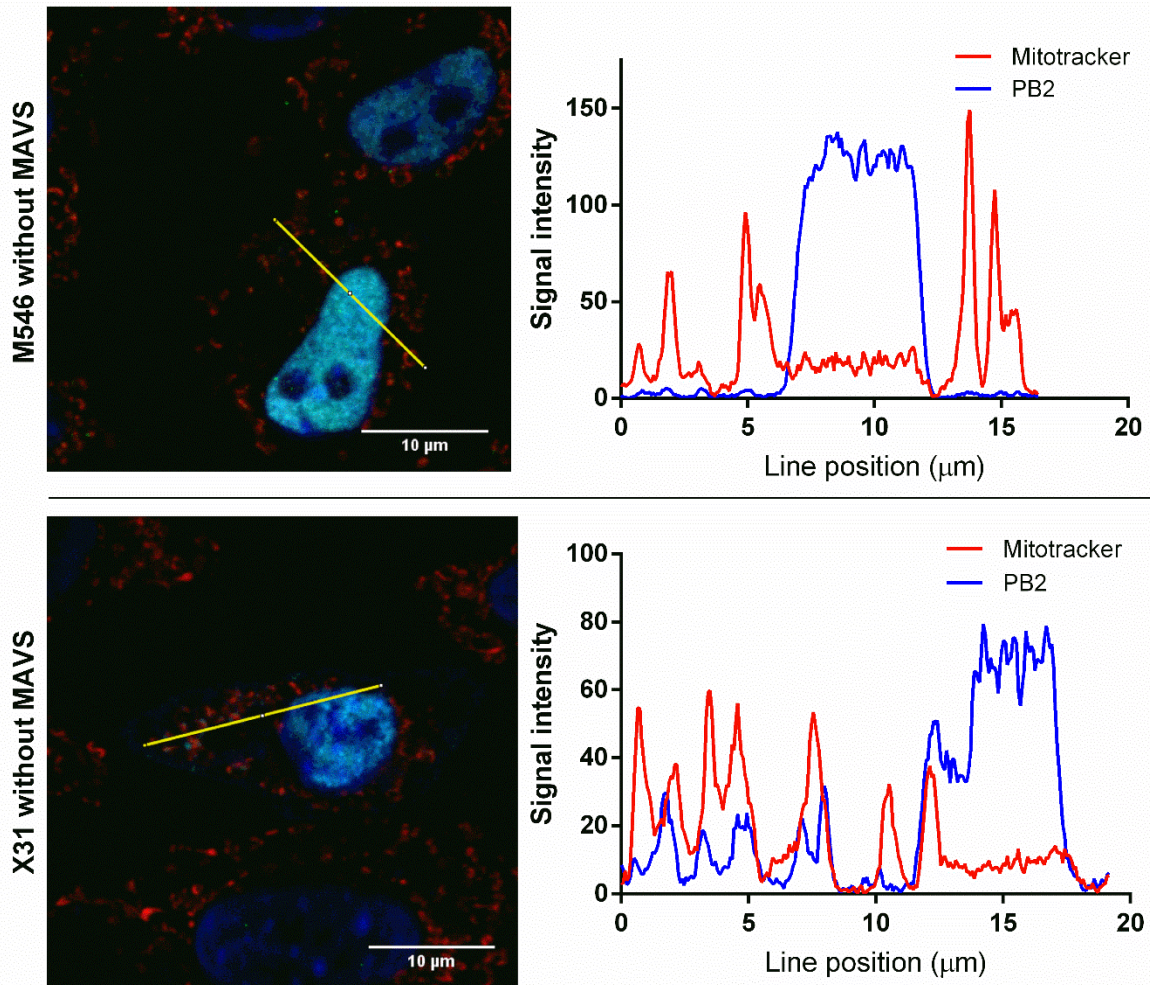


Figure 12. Localization of PB2 and DF-1 cell mitochondria. PB2 from the avian IAV strain M546 does not localize with DF-1 mitochondria, while mammalian PB2 from the IAV strain X31 displays an increase in mitochondrial association. Confocal images and signal intensity plots are shown depicting the cellular localization of DF-1 cell mitochondria (red) and influenza PB2 proteins (blue) within DF-1 cells. Each cellular image is a representative picture from 8 analyzed cells. A yellow line has been drawn in each image to indicate the location of the signal intensity plot. An average of three pixels was used to generate the signal intensity plot after background noise was subtracted from all images using the Rolling Ball Background Subtraction tool within ImageJ. The scale bar represents a 10 μm length within each image.

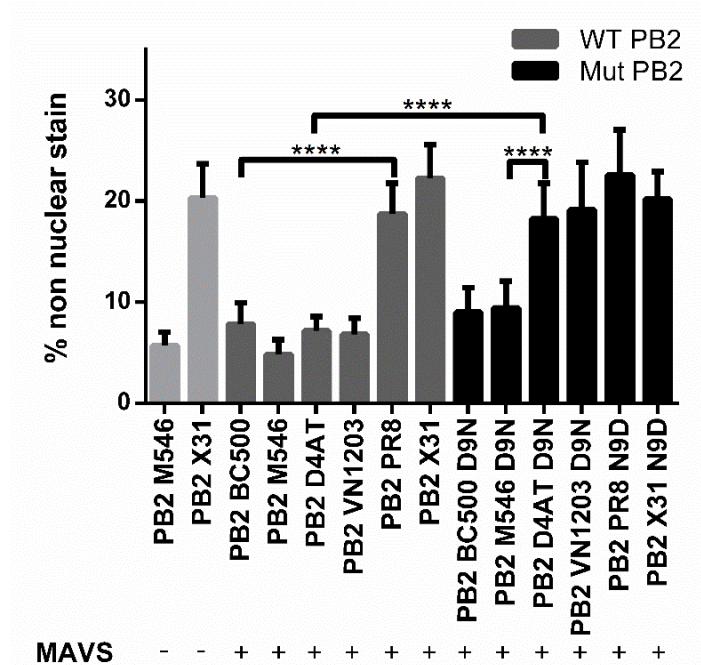


Figure 13. Percent non-nuclear PB2 staining in DF-1 cells. The residue at position 9 is not the sole determinant of PB2 non-nuclear staining within DF-1 cells. PB2 signals from the confocal images in Figure 11 were analyzed by measuring the sum of pixel intensity (raw integrated density) for PB2 staining within and outside of DF-1 nuclei using ImageJ. The difference between the PB2 whole cell signal and nuclear signal was then plotted as a percent of the total signal and described as non-nuclear staining. Background noise was subtracted from all images using the Rolling Ball Background Subtraction tool within ImageJ. Mean values were calculated from the average of 8 analyzed cells for each treatment (n=8). Error bars represent the standard deviation from the mean. A one-way ANOVA was conducted to compare the cytoplasmic staining of differentially adapted WT and mutant PB2 proteins. There was a significant effect on PB2 cytoplasmic staining ($F[13,98] = 44.66, p < 0.0001$). **** indicates a P value < 0.0001 , based on a Tukey multiple comparison test.

Chapter 4. Discussion

Activated MAVS proteins form filaments, which are crucial to their cellular function, as studies have shown the formation of MAVS filaments are strongly correlated with the activation of IFN- β signaling downstream of MAVS (74, 75). Some models have tried to explain how RIG-I nucleates MAVS filament formation (81, 95–97), however, structural investigation has not strongly supported the proposed models. Therefore, I was very fortunate to have the opportunity to collaborate with the Sun Hur research group and test their model of RIG-I-MAVS activation in an avian cell culture system. Here I have shown that key mutations in the interfaces between duck RIG-I and MAVS, as predicted by the Sun Hur model, have partially abrogated and restored MAVS signaling and filament formation in avian cells.

4.1 The RIG-I-MAVS filament nucleation event is transient.

It is known that both duck RIG-I and MAVS cannot activate the MAVS-mediated IFN signaling pathway in human cells. Similarly, both human RIG-I and MAVS cannot activate the MAVS-mediated IFN signaling pathway in avian cells. Therefore, an accurate model of RIG-I-MAVS IFN signal activation should be able to predict key residues in duck RIG-I that when mutated can restore IFN signal activation in a human system. Here, the Sun Hur group was able to demonstrate just that, with the mutation of T175K/T176E in the duck 2CARD of RIG-I. Interestingly, I found the T175K/T176E in duck 2CARD^{RIG-I} did not abrogate the IFN signal in avian cells, which could suggest the nucleation interaction between the 2CARD of RIG-I and the CARD of MAVS is flexible and can withstand changes to some of the key interacting residues. A flexible or transient nucleation interaction between RIG-I and MAVS would be advantageous to an infected cell, as this would allow for multiple MAVS filaments to be initiated from one

RIG-I 2CARD tetramer. This would quickly amplify the antiviral IFN signal and lead to a quick and efficient activation of the innate immune response, potentially protecting other cells from viral infection.

4.2 MAVS filament formation is conserved across species.

The CARD of MAVS has poor sequence conservation between human and duck MAVS, specifically at key residues in the inter-CARD interface within the MAVS filament.

Interestingly, the CARD domains from MAVS were shown, by the Sun Hur research group, to form filaments despite major MAVS residue differences. In an attempt to test the Sun Hur model of MAVS filament formation, functional mutations were performed on key MAVS interface residues to abrogate the IFN signal in both duck and human MAVS. I found that the predicted mutations of Y56R and H43D completely inhibited the duck MAVS-mediated IFN signal. This suggests the Sun Hur model of MAVS filament formation is conserved in ducks, as mutations in the predicted residues completely abrogated the IFN signal. However, I found that charge complementary mutations at these duck MAVS residues did not significantly restore the IFN signal. This is most likely caused by the abnormal MAVS filament structures shown by the Sun Hur research group, as downstream adaptor proteins would have a difficult time interacting with the abnormal mutant MAVS filament surface. Together, these results suggest that the RIG-I nucleated MAVS filament structure is a conserved cross species mechanism of IFN signaling. However, the filament mechanism of signal transduction may not be limited to the RIG-I-MAVS pathway. Recently, the sensory proteins AIM2 and NLRP3, which activate inflammasomes, have also been shown to nucleate CARD filaments from the downstream adaptor protein ASC (98). Therefore, it appears the structural mechanism of CARD filament formation may be conserved

across several innate immune receptors, and would be an excellent target for viral proteins to shut down the innate antiviral response.

4.3 Influenza PB2 inhibition of MAVS IFN signaling

PB2-MAVS interactions are known to dampen the antiviral IFN response in IAV infected cells (8, 9), and therefore, PB2 inhibition of MAVS IFN signaling is thought to affect IAV virulence and fitness. Differences in IFN inhibition have arisen between mammalian and avian adapted IAV PB2 proteins (80). I hypothesized this difference in IFN inhibition is caused by the selective pressure for PB2 to adapt and inhibit MAVS molecules from different species. Therefore, avian IAV PB2 should be better adapted than mammalian PB2 to inhibit and interact with duck MAVS in avian cells. Here, I have examined the structure, function, and localization of 6 PB2 proteins from 4 avian (BC500, M546, D4AT, VN1203) and 2 mammalian (PR8 and X31) adapted IAV strains within avian cells. Unexpectedly, I found mammalian adapted PB2 proteins to be a more potent inhibitor of avian IFN- β signaling, as compared to avian adapted PB2s. Additionally, I found the PB2 inhibition of IFN in avian cells is partially dependent on both PB2-MAVS binding interactions and PB2 localization. Together, my findings suggest mammalian IAV PB2 proteins have acquired a cross species ability to inhibit IFN, which could have the potential to affect both IAV virulence and fitness.

4.4 Mammalian adapted PB2 is a potent cross species inhibitor of IFN- β

Mammalian IAV adapted PB2 proteins are more potent inhibitors of duck MAVS-mediated IFN- β signaling than avian adapted PB2 proteins. This observation is contrary to what has been reported in the literature. In mammalian cells (HEK293), PB2 proteins from mammalian adapted IAVs (PR8 and WSN) were shown to be ~50% more effective than PB2 from avian adapted

IAVs (A/Hong Kong/483/34 and A/Hong Kong/486/34) at inhibiting the IFN- β promoter activity (9). Similarly in avian chicken cells (DF-1), a PB2 protein from a chicken adapted IAV (A/chicken/Yamaguchi/7/04) was reported to be ~30% more effective than a PB2 protein from a duck adapted IAV (A/duck/Hokkaido/Vac-1/04) at inhibiting the IFN- β promoter activity (99). From this, it appeared IAV PB2 proteins from different strains are adapting to inhibit a familiar interaction partner in these cellular systems, I suspected it was the host MAVS protein. In contrast, I have found that mammalian adapted PB2 proteins are capable of having a potent IFN inhibition effect across the avian-mammalian species barrier. This could suggest mammalian adapted PB2 proteins are adapting to interact with a conserved MAVS signaling structure and not specific MAVS surface residues. Two potential PB2 interacting structures could be the conserved CARD^{MAVS} filament (72), or a smaller conserved secondary structure such as the conserved α -helixes within the CARD of MAVS proteins. Since I have observed mammalian adapted IAV PB2 to partially localize with mitochondria in the absence of activated MAVS filaments in chicken cells, it is more probable that PB2 is interacting with smaller conserved MAVS secondary structures. However to test this proposition would require further functional work and most likely a crystal structure to confirm the true PB2 interacting domain of MAVS, as current research as only narrowed the PB2 interacting domains of MAVS to the first 150 N-terminal residues (79). Nonetheless, for the remainder of my discussion I will discuss the differences in IAV PB2 IFN inhibition with regards to PB2 structure, MAVS binding, and PB2 localization.

4.5 PB2 displays three adaptive residues, which form a cleft like structure near the MAVS binding domain.

I used protein modelling software and the recently published IAV PB2 X-ray crystal structure (91), to model and annotate where adaptive residues (80) are located within the PB2 structure. In agreement with previous results (79), I found the important adaptive residue 9 of PB2, mapped to the first N-terminal helix within the MAVS binding domain. However, two other adaptive PB2 residues (64 and 81) were found to map near the same region as residue 9. Based on their position and shared potential interaction surface, these residues may interact with a common molecule. This is significant as it is the first report of the structural possibility for these three PB2 residues (9, 64, 81) to be involved in MAVS-PB2 interactions. Specifically, the structural position of the bottom α -helix, which contains residue 9, and the upper surface structure made by PB2 residues 64 – 81, provide a cleft where it is conceivable to fit an α -helix from an interacting protein, such as α -helixes from the MAVS CARD. Furthermore, a conserved MAVS binding cleft partially composed from three adaptive residues within the PB2 protein could help explain the differences in IFN inhibition seen between LPAI, HPAI, and mammalian adapted PB2 proteins. It has been shown that the strongly conserved third N-terminal α -helix of PB2 mediates the majority of MAVS interactions (79), however this fails to explain why differentially adapted PB2 proteins from different IAV strains display varying degrees of MAVS binding. Therefore a cleft composed of several adaptive PB2 residues which influence PB2-MAVS binding would be a more plausible explanation for why differentially adapted IAV PB2 proteins display varying abilities to bind MAVS and inhibit the IFN response. Specifically, future research may want to investigate PB2 residue 64 as three different residues are expressed between the sampled LPAI

(M), HPAI (I), and mammalian adapted (T) IAV strains. However, for the remainder of my discussion, I will focus on the effects of PB2 residue 9 and the PB2-MAVS interaction.

4.6 PB2-mediated IFN inhibition is partially dependent on PB2-MAVS interactions.

In order to investigate the functional significance of PB2-MAVS interactions on IFN inhibition, I analyzed each PB2-MAVS interaction by immunoprecipitation. I found that LPAI adapted PB2 proteins have a reduced capacity to bind duck MAVS. In particular, PB2 from M546 displayed no detectable amount of PB2-MAVS binding. This is extremely interesting as it is the first reported case of a PB2 protein that does not interact with MAVS. It also helps explain the significantly reduced IFN inhibition capability of this PB2 protein, suggesting that PB2 binding is partially responsible for an effective inhibition of MAVS-mediated IFN signaling. Until recently, all examined PB2 proteins have been reported to interact with MAVS, regardless of the IAV strain (8, 9, 79). However, this negative PB2 binding result is puzzling, as there are no residue differences between the BC500 PB2 and the M546 PB2 within the MAVS binding domain or my proposed binding cleft which involves PB2 residues 9, 64, and 81. This led me to ask, what then, is causing this difference in MAVS binding? It has been shown that residues upstream of PB2 residue 119 are still capable of mediating limited PB2-MAVS interaction (9), therefore I propose that PB2 could also contain other residues that influence MAVS binding outside of both the characterized N-terminal MAVS binding domain (79) and my proposed PB2 binding cleft. Residues G123 and I186 are the first N-terminal residues which differ from the BC500 PB2 protein and are unique to the IAV strain M546. Both G123 and I186 are not conserved among other IAV strains and are not considered to be avian or human adaptive IAV residues. However G123 and I186 are both located within surface accessible α -helices, which would allow them to participate in intermolecular interactions, potentially influencing the PB2-

MAVS interaction. Although it would seem difficult for PB2 residues G123 and I186 to have a direct interaction with duck MAVS, due to the large modeled distance from the required MAVS binding domain, this does not eliminate the possibility of these residues playing an indirect role in PB2-MAVS binding. Perhaps uncharacterized cellular adaptor proteins can also interact with downstream PB2 residues (G123 or I186) that modify the PB2-MAVS interaction. In this way surface accessible PB2 residues further downstream from the MAVS binding site could modify the observed PB2-MAVS interactions. Therefore G123 and I186 in M546 would be excellent early candidates for potential future research that investigates other PB2 residues that could directly or indirectly affect PB2-MAVS binding.

PB2 residue 9 is known to affect both IFN inhibition and PB2 localization (8), and I suspect it also influences PB2-MAVS binding interactions. To investigate the role of the species adapted PB2 residue 9 in MAVS-PB2 interactions, I swapped the avian adaptive residues (D9) and the mammalian adaptive residues (N9) with each other (D9N and N9D), and I tested for direct or indirect protein interactions by immunoprecipitation. I established that a D9N mutation in the PB2 from M546 restored PB2-MAVS interactions and as expected, increased the IFN inhibition of this PB2 M546 mutant. However this same mutation in the other LPAI, HPAI, and mammalian adapted PB2 proteins did not significantly change their observed PB2-MAVS binding interactions, and actually decreased IFN inhibition. Therefore, it appears the mammalian adaptive residue at position 9, asparagine, can improve MAVS binding and IFN inhibition; however, it is not the sole determinant of PB2 function. In fact, PB2 residue 9 may be working cooperatively with other PB2 residues. I have presented a structural model that suggests PB2 residues 64 and 81 could be involved in determining the PB2-MAVS interaction, and therefore a

change to only one residue within the PB2 MAVS binding cleft could cause a significant change that influences PB2 function, however additional PB2 residue changes seem to be required to transfer mammalian adapted PB2 function to avian PB2 proteins. Therefore, together these results provide support that multiple PB2 residues are important for either direct or indirect PB2-MAVS interactions, however I cannot rule out that these adaptive residues are not also modifying the location of PB2 within DF-1 cells.

4.7 PB2-mediated IFN inhibition is partially dependent on PB2 localization.

PB2 has long been characterized to localize to the mitochondria (77, 78), and more recently mammalian adapted PB2 has been described to localize to the mitochondria while interacting with human MAVS (8, 79). To investigate how these differently adapted PB2 proteins localize in avian cells, I used fluorescent confocal microscopy to characterize the location of PB2 and duck MAVS. I discovered that only mammalian adapted PB2 proteins showed a partial localization with duck MAVS, while avian adapted PB2s did not. Although this is not concrete quantitative co-localization data, this observation does agree with other work and shows a similar trend as mammalian PB2 has been shown to localize to the mitochondria (8). However, it was expected that due to specific adaptive mutation in PB2, avian adapted PB2 would be better suited to interact with avian MAVS. Thus, it appears mammalian adapted PB2 has evolved an increased ability to localize with MAVS, which may explain why mammalian adapted PB2 proteins inhibit IFN signaling to a greater extent than avian adapted PB2 in avian cells. In fact, it could be a combination of PB2-MAVS binding interactions and PB2 localization that both have an effect on PB2 function, as differences in both PB2 localization and MAVS binding coincide with differences in PB2 IFN signaling inhibition.

To understand what drives this adaptive localization function in PB2, I again swapped the avian adaptive residues (D9) and the mammalian adaptive residues (N9) with each other (D9N and N9D) and observed the mutated PB2 localization with regards to duck MAVS in DF-1 cells. Surprisingly, a D9N (avian to mammalian) mutation in avian adapted PB2 did not grant the ability for avian adapted PB2 to localize with duck MAVS, as was previously described (8). The mutations instead produced different staining phenotypes between LPAI and HPAI PB2 proteins, where HPAI PB2 became more cytoplasmic and LPAI PB2 barely differed in its PB2 staining pattern. This could suggest PB2 localization is dependent on several PB2 residues, as one residue change is not sufficient to transfer the mammalian adapted PB2 function to avian PB2 proteins. Interestingly, I speculate that mutated HPAI PB2s could be interacting with cellular adaptor proteins, which would allow HPAI PB2s to be targeted outside of the nucleus. Conversely, the mutated LPAI PB2s could lack other key residue mutations, which would prevent them from interacting with potential cellular adaptor proteins and cause them to remain solely targeted to the nucleus. Therefore, further research would be needed to investigate the effect of other mammalian adaptive PB2 mutations on PB2 localization. Here I have suggested residues 64 and 81 of PB2 would be prime candidates for future research as I have found them to share a potential binding cleft with PB2 residue 9, which is a PB2 residue known to affect PB2 localization (8).

Additionally, an N9D mutation in mammalian adapted PB2 abrogated any significant PB2 localization to MAVS, and caused significant non-localized cytoplasmic PB2 staining. Again, this could suggest that other PB2 residues are necessary for localizing PB2 outside of the nucleus, however the human adaptive PB2 residue N9 is required in combination with other

residues to specifically target PB2 to MAVS. Together, these results indicate that the mammalian adaptive residue N9 in avian adapted PB2 is not sufficient to confer PB2 localization to MAVS, but it is required for mammalian adapted PB2 to localize to the mitochondria. Therefore, it appears that mammalian adapted IAV PB2 proteins have acquired several adaptive mutations that function cooperatively to interact and localize with the generally conserved MAVS structure. However, the exact selective advantage this increased IFN inhibition confers to mammalian adapted IAVs remains to be discussed.

4.8 PB2-mediated IFN inhibition could increase viral fitness for mammalian adapted IAVs.

Initially, the accepted theory on pathogen evolution and virulence was that asymptomatic disease is the eventual evolutionary result of prolonged host-pathogen interactions, as harm to the host decreases the pathogen's fitness (100, 101). This theory works well for asymptomatic IAV infections in ducks, as they are the natural host of IAVs, and have most likely co-evolved with the virus to create a reservoir that ensures both the virus and the host survive (25). However, this theory fails to explain the persistent symptomatic IAV infections we see in humans during our annual "flu season", as well as why viruses mutate to produce the occasional highly pathogenic pandemics, such as the 1918 (H1N1), 1957 (H2N2), and 1968 (H3N2) IAV pandemics (31–33). Here, I speculate that IAV virulence behaves in a way that is best explained by the transmission-virulence trade-off hypothesis (102, 103), which argues that virulence can be adaptive to a certain extent when its benefits are linked to other beneficial pathogen traits such as increased transmission. HIV in humans is a prime example of this hypothesis at work, as there is a positive relationship between HIV transmissibility and viral load, but optimal HIV transmission occurs at intermediate viral loads (104). In the case of avian adapted IAV infections in ducks, I speculate

that there is no selective pressure for the virus to cause disease. IAVs replicate asymptotically in the intestinal tract of ducks and are excreted in high volumes into the environment via fecal contaminated lake water, which can then cause infections in other animals (26). This transmission strategy employed by avian IAVs is very efficient and causes minimal cost to the host as intestinal epithelial cells turn over quite frequently. Thus, there has been no need for avian influenza to develop virulence to improve viral fitness, as this is the perfect host for IAV infection. However, in humans the situation is quite different, IAV infection typically occurs in the lungs (105), and as one can imagine, human IAV transmission would be difficult if humans did not sneeze and cough during an upper respiratory tract infection. Therefore, it could be advantageous for mammalian adapted viruses to evolve pathogenic mechanisms that improve viral replication and transmission, such as IFN inhibition. Although I have not measured the actual amount of IFN- β expressed in my DF-1 cell experiments, highly active promoters can greatly upregulate the amount of mRNA transcripts, which are known to correlate more strongly with levels of protein expression than steady-state levels of mRNA transcripts (106). Therefore I feel confident that changes to a highly active IFN- β promoter is affecting the amount of expressed IFN- β . However, further investigation would be needed to ascertain that PB2 inhibition of IFN signaling is indeed affecting IFN- β expression levels. In reference to PB2, one study demonstrated the HA and NA proteins from the 1918 influenza pandemic strain were not sufficient to produce respiratory droplet transmission in an avian IAV strain in ferrets, but the addition of the 1918 influenza PB2 protein was able to confer this ability (107). Additionally, a mammalian adapted IAV expressing the avian adapted PB2 residue (D9) was significantly attenuated in mice, compared to the wild type strain (8). Through these examples, it is apparent that PB2 and specifically changes at PB2 residue 9 can play an integral role in IAV transmission

and fitness. Therefore, I speculate that the effective IFN inhibition displayed by mammalian adapted PB2 proteins, could be an adaptation acquired to improve mammalian influenza viral fitness.

4.9 Conclusions

In summary, I have helped demonstrate that the RIG-I-MAVS IFN signaling mechanism could be conserved across different species, which would make it an ideal target for IAV proteins like PB2. Additionally, I found mammalian adapted IAV PB2 has potentially acquired a cross species ability to be a potent IFN inhibitor in avian cells. This IFN inhibition is also shown to be partially dependent on both PB2-MAVS binding interactions and PB2 localization. Furthermore, I have found that mammalian adapted PB2 residue N9 is required for PB2 functions, such as PB2-MAVS binding, localization, and IFN inhibition, but it is not sufficient to transfer all these functions to avian adapted PB2 proteins. As a result, PB2 residues 64 and 81 could be additional sources of variation in PB2 that cause functional differences between IAV strains, as they share a potential common binding cleft with the adaptive residue 9 of PB2. Unfortunately, the exact mechanism of how PB2 mediates the inhibition of MAVS-mediated IFN signaling is still unknown. However since truncated PB2 interactions with MAVS increases MAVS-mediated IFN signaling (7), it appears that a direct or indirect PB2 interaction with MAVS is not the cause of IFN inhibition. Thus, it could be the steric hindrance of full length PB2 that is either blocking the nucleation of MAVS filaments or blocking the binding of downstream adaptors, which is causing the IFN signaling inhibition. However, to determine the exact mechanism of PB2 IFN inhibition would require further study. Here, I have highlighted my results and findings as it is important to identify and investigate all adaptive mutations that could be associated with

elevated IAV virulence and viral fitness within mammals. This will allow us to better estimate the risk that avian IAVs pose to human health.

References

1. **Bouvier NM, Palese P.** 2008. The biology of influenza viruses. *Vaccine* **26**(4):49–53.
2. **Szewczyk B, Bieńkowska-szewczyk K, Król E.** 2014. Introduction to molecular biology of influenza A viruses. *ACTA Biochimica Polonica* **61**(3):397–401.
3. **Chen W, Calvo PA, Malide D, Gibbs J, Schubert U, Bacik I, Basta S, O’Neill R, Schickli J, Palese P, Henklein P, Bennink JR, Yewdell JW.** 2001. A novel influenza A virus mitochondrial protein that induces cell death. *Nature Medicine* **7**(12):1306–1312.
4. **Wise HM, Foeglein A, Sun J, Dalton RM, Patel S, Howard W, Anderson EC, Barclay WS, Digard P.** 2009. A complicated message: Identification of a novel PB1-related protein translated from influenza A virus segment 2 mRNA. *Journal of Virology* **83**(16):8021–8031.
5. **Jagger BW, Wise HM, Kash JC, Walters KA, Wills NM, Xiao YL, Dunfee RL, Schwartzman LM, Ozinsky A, Bell GL, Dalton RM, Lo A, Efstathiou S, Atkins JF, Firth AE, Taubenberger JK, Digard P.** 2012. An overlapping protein-coding region in influenza A virus segment 3 modulates the host response. *Science* **337**(6091):199–204.
6. **Muramoto Y, Noda T, Kawakami E, Akkina R, Kawaoka Y.** 2013. Identification of novel influenza A virus proteins translated from PA mRNA. *Journal of Virology* **87**(5):2455–2462.
7. **Boergeling Y, Rozhdestvensky TS, Schmolke M, Resa-Infante P, Robeck T, Randau G, Wolff T, Gabriel G, Brosius J, Ludwig S.** 2015. Evidence for a novel mechanism of influenza virus-induced type I interferon expression by a defective RNA-encoded protein. *PLOS Pathogens* **11**(5):1–25.
8. **Graef KM, Vreede FT, Lau YF, McCall AW, Carr SM, Subbarao K, Fodor E.** 2010. The PB2 subunit of the influenza virus RNA polymerase affects virulence by interacting with the mitochondrial antiviral signaling protein and inhibiting expression of beta interferon. *Journal of Virology* **84**(17):8433–8445.
9. **Iwai A, Shiozaki T, Kawai T, Akira S, Kawaoka Y, Takada A, Kida H, Miyazaki T.** 2010. Influenza A virus polymerase inhibits type I interferon induction by binding to interferon β promoter stimulator 1. *Journal of Biological Chemistry* **285**(42):32064–32074.
10. **Skehl JJ, Wiley DC.** 2000. Receptor binding and membrane fusion in virus entry: the influenza hemagglutinin. *Annual Review Biochemistry* **69**:531–69.
11. **Lakadamyali M, Rust MJ, Zhuang X.** 2004. Endocytosis of influenza viruses. *Microbes Infect* **6**(10):929–936.

12. **Stegmann T.** 2000. Membrane fusion mechanisms: the influenza hemagglutinin paradigm and its implications for intracellular fusion. *Traffic* **1**(8):598–604.
13. **Martin K, Helenius A.** 1991. Transport of incoming influenza virus nucleocapsids into the nucleus. *Journal of Virology* **65**(1):232–244.
14. **Cros JF, Palese P.** 2003. Trafficking of viral genomic RNA into and out of the nucleus: Influenza, Thogoto and Borna disease viruses. *Virus Research* **95**:3–12.
15. **Engelhardt O, Smith M, Fodor E.** 2005. Association of the influenza A virus RNA-dependent RNA polymerase with cellular RNA polymerase II. *Journal of Virology* **79**(9):5812–5818.
16. **Fechter P, Mingay L, Sharps J, Chambers A, Fodor E, Brownlee GG.** 2003. Two aromatic residues in the PB2 subunit of influenza A RNA polymerase are crucial for cap binding. *Journal of Biological Chemistry* **278**(22):20381–20388.
17. **Dias A, Bouvier D, Crépin T, McCarthy AA, Hart DJ, Baudin F, Cusack S, Ruigrok RWH.** 2009. The cap-snatching endonuclease of influenza virus polymerase resides in the PA subunit. *Nature* **458**(7240):914–918.
18. **Huang X, Liu T, Muller J, Levandowski RA, Ye Z.** 2001. Effect of influenza virus matrix protein and viral RNA on ribonucleoprotein formation and nuclear export. *Virology* **287**(2):405–416.
19. **O'Neill RE, Talon J, Palese P.** 1998. The influenza virus NEP (NS2 protein) mediates the nuclear export of viral ribonucleoproteins. *EMBO Journal* **17**(1):288–296.
20. **Leser GP, Lamb RA.** 2005. Influenza virus assembly and budding in raft-derived microdomains: A quantitative analysis of the surface distribution of HA, NA and M2 proteins. *Virology* **342**(2):215–227.
21. **Barman S, Ali A, Hui EKW, Adhikary L, Nayak DP.** 2001. Transport of viral proteins to the apical membranes and interaction of matrix protein with glycoproteins in the assembly of influenza viruses. *Virus Research* **77**(1):61–69.
22. **Noton SL, Medcalf E, Fisher D, Mullin AE, Elton D, Digard P.** 2007. Identification of the domains of the influenza A virus M1 matrix protein required for NP binding, oligomerization and incorporation into virions. *Journal of General Virology* **88**(8):2280–2290.
23. **Palese P, Tobita K, Ueda M, Compans RW.** 1974. Characterization of temperature sensitive influenza virus mutants defective in neuraminidase. *Virology* **61**(2):397–410.
24. **Tong S, Zhu X, Li Y, Shi M, Zhang J, Bourgeois M, Yang H, Chen X, Recuenco S, Gomez J, Chen LM, Johnson A, Tao Y, Dreyfus C, Yu W, McBride R, Carney PJ,**

- Gilbert AT, Chang J, Guo Z, Davis CT, Paulson JC, Stevens J, Rupprecht CE, Holmes EC, Wilson IA, Donis RO.** 2013. New world bats harbor diverse influenza A viruses. *PLOS Pathogens* **9**(10):1–12.
25. **Webster R, Bean W, Gorman O, Chambers T, Kawaoka Y.** 1992. Evolution and ecology of influenza A viruses. *Microbiological Reviews* **56**(1):152–179.
 26. **Webster RG, Yakhno M, Hinshaw VS, Bean WJ, Murti KG.** 1978. Intestinal influenza: replication and characterization of influenza viruses in ducks. *Virology* **84**(2):268–278.
 27. **Neumann G, Kawaoka Y.** 2015. Transmission of influenza A viruses. *Virology* **480**:234–246.
 28. **OIE.** 2015. Manual of diagnostic tests and vaccines for terrestrial animals. Paris, France.
 29. **Bevins SN, Pedersen K, Lutman MW, Baroch JA, Schmit BS, Kohler D, Gidlewski T, Nolte DL, Swafford SR, DeLiberto TJ.** 2014. Large-scale avian influenza surveillance in wild birds throughout the United States. *PLOS One* **9**(8):1–8.
 30. **Qi L, Davis AS, Jagger BW, Schwartzman LM, Dunham EJ, Kash JC, Taubenberger JK.** 2012. Analysis by single-gene reassortment demonstrates that the 1918 influenza virus is functionally compatible with a low-pathogenicity avian influenza virus in mice. *Journal of Virology* **86**(17):9211–9220.
 31. **Taubenberger JK, Morens DM.** 2006. 1918 Influenza: The mother of all pandemics. *Emerging Infectious Diseases* **12**(1):15–22.
 32. **Kilbourne ED.** 2006. Influenza pandemics of the 20th century. *Emerging Infectious Diseases* **12**(1):9–14.
 33. **Scholtissek C, Rohde W, Von Hoyningen V, Rott R.** 1978. On the origin of the human influenza virus subtypes H2N2 and H3N2. *Virology* **87**(1):13–20.
 34. **Dawood FS, Iuliano AD, Reed C, Meltzer MI, Shay DK, Cheng PY, Bandaranayake D, Breiman RF, Brooks WA, Buchy P, Feikin DR, Fowler KB, Gordon A, Hien NT, Horby P, Huang QS, Katz MA, Krishnan A, Lal R, Montgomery JM, Mølbak K, Pebody R, Presanis AM, Razuri H, Steens A, Tinoco YO, Wallinga J, Yu H, Vong S, Bresee J, Widdowson MA.** 2012. Estimated global mortality associated with the first 12 months of 2009 pandemic influenza A H1N1 virus circulation: A modelling study. *Lancet Infectious Diseases* **12**(9):687–695.
 35. **Garten RJ, Davis CT, Russell CA, Shu B, Lindstrom S, Balish A, Sessions WM, Xu X, Skepner E, Deyde V, Okomo-Adhiambo M, Gubareva L, Barnes J, Smith CB, Emery SL, Hillman MJ, Rivaller P, Smagala J, DeGraaf M, Burke DF, Fouchier RAM, Pappas C, Alpuche-Aranda CM, López-Gatell H, Olivera H, López I, Myers**

- CA, Faix D, Blair PJ, Yu C, Keene KM, Dotson PD, Boxrud D, Sambol AR, Abid SH, George K St., Bannerman T, Moore AL, Stringer DJ, Blevins P, Demmler-Harrison GJ, Ginsberg M, Kriner P, Waterman S, Smole S, Guevara HF, Belongia EA, Clark PA, Beatrice ST, Donis R, Katz J, Finelli L, Bridges CB, Shaw M, Jernigan DB, Uyeki TM, Smith DJ, Klimov AI, Cox NJ. 2009. Antigenic and genetic characteristics of the early isolates of swine-origin 2009 A(H1N1) influenza viruses circulating in humans. *Science* **325**(5937):197–201.
36. **Klenk HD, Rott R, Orlich M, Blödorn J.** 1975. Activation of influenza A viruses by trypsin treatment. *Virology* **68**(2):426–439.
37. **Rott R, Klenk HD, Nagai Y, Tashiro M.** 1995. Influenza viruses, cell enzymes, and pathogenicity. *American Journal of Respiratory and Critical Care Medicine* **152**(4):516–519.
38. **Schrauwen EJA, Herfst S, Leijten LM, van Run P, Bestebroer TM, Linster M, Bodewes R, Kreijtz JHCM, Rimmelzwaan GF, Osterhaus ADME, Fouchier RAM, Kuiken T, van Riel D.** 2012. The multibasic cleavage site in H5N1 virus is critical for systemic spread along the olfactory and hematogenous routes in ferrets. *Journal of Virology* **86**(7):3975–3984.
39. **Suguitan a. L, Matsuoka Y, Lau YF, Santos CP, Vogel L, Cheng LI, Orandle M, Subbarao K.** 2012. The multibasic cleavage site of the hemagglutinin of highly pathogenic A/Vietnam/1203/2004 (H5N1) avian influenza virus acts as a virulence factor in a host-specific manner in mammals. *Journal of Virology* **86**(5):2706–2714.
40. **Schrauwen EJA, Bestebroer TM, Munster VJ, de Wit E, Herfst S, Rimmelzwaan GF, Osterhaus ADME, Fouchier RAM.** 2011. Insertion of a multibasic cleavage site in the haemagglutinin of human influenza H3N2 virus does not increase pathogenicity in ferrets. *Journal of General Virology* **92**(6):1410–1415.
41. **Schrauwen EJ, Fouchier RA.** 2014. Host adaptation and transmission of influenza A viruses in mammals. *Emerging Microbes & Infections* **3**(2):1–10.
42. **Van Riel D, Leijten LME, De Graaf M, Siegers JY, Short KR, Spronken MIJ, Schrauwen EJA, Fouchier RAM, Osterhaus ADME, Kuiken T.** 2013. Novel avian-origin influenza A (H7N9) virus attaches to epithelium in both upper and lower respiratory tract of humans. *American Journal of Pathology* **183**(4):1137–1143.
43. **Shinya K, Ebina M, Yamada S, Ono M, Kasai N, Kawaoka Y.** 2006. Avian flu: influenza virus receptors in the human airway. *Nature* **440**(7083):435–436.
44. **Wagner R, Matrosovich M, Klenk HD.** 2002. Functional balance between haemagglutinin and neuraminidase in influenza virus infections. *Reviews in Medical Virology* **12**(3):159–166.

45. **Fouchier RAM, Schneeberger PM, Rozendaal FW, Broekman JM, Kemink SAG, Munster V, Kuiken T, Rimmelzwaan GF, Schutten M, Van Doornum GJJ, Koch G, Bosman A, Koopmans M, Osterhaus ADME.** 2004. Avian influenza A virus (H7N7) associated with human conjunctivitis and a fatal case of acute respiratory distress syndrome. *Proc Natl Acad Sci U S A* **101**(5):1356–1361.
46. **De Wit E, Munster VJ, van Riel D, Beyer WEP, Rimmelzwaan GF, Kuiken T, Osterhaus ADME, Fouchier RAM.** 2010. Molecular determinants of adaptation of highly pathogenic avian influenza H7N7 viruses to efficient replication in the human host. *Journal of Virology* **84**(3):1597–1606.
47. **Matsuoka Y, Swayne DE, Thomas C, Rameix-Welti MA, Naffakh N, Warnes C, Altholtz M, Donis R, Subbarao K.** 2009. Neuraminidase stalk length and additional glycosylation of the hemagglutinin influence the virulence of influenza H5N1 viruses for mice. *Journal of Virology* **83**(9):4704–4708.
48. **García-Sastre A.** 2011. Induction and evasion of type I interferon responses by influenza viruses. *Virus Research* **162**:12–18.
49. **García-Sastre A, Egorov A, Matassov D, Brandt S, Levy DE, Durbin JE, Palese P, Muster T.** 1998. Influenza A virus lacking the NS1 gene replicates in interferon-deficient systems. *Virology* **252**(2):324–330.
50. **Nemeroff ME, Barabino SM, Li Y, Keller W, Krug RM.** 1998. Influenza virus NS1 protein interacts with the cellular 30 kDa subunit of CPSF and inhibits 3'end formation of cellular pre-mRNAs. *Molecular Cell* **1**(7):991–1000.
51. **Twu KY, Kuo RL, Marklund J, Krug RM.** 2007. The H5N1 influenza virus NS genes selected after 1998 enhance virus replication in mammalian cells. *Journal of Virology* **81**(15):8112–8121.
52. **Hale BG, Steel J, Medina RA, Manicassamy B, Ye J, Hickman D, Hai R, Schmolke M, Lowen AC, Perez DR, García-Sastre A.** 2010. Inefficient control of host gene expression by the 2009 pandemic H1N1 influenza A virus NS1 protein. *Journal of Virology* **84**(14):6909–6922.
53. **Baigent SJ, McCauley JW.** 2003. Influenza type A in humans, mammals and birds: Determinants of virus virulence, host-range and interspecies transmission. *BioEssays* **25**(7):657–671.
54. **Maier HJ, Kashiwagi T, Hara K, Brownlee GG.** 2008. Differential role of the influenza A virus polymerase PA subunit for vRNA and cRNA promoter binding. *Virology* **370**(1):194–204.

55. **Sanz-Ezquerro JJ, Zürcher T, de la Luna S, Ortín J, Nieto A.** 1996. The amino-terminal one-third of the influenza virus PA protein is responsible for the induction of proteolysis. *Journal of Virology* **70**(3):1905–1911.
56. **Yuan P, Bartlam M, Lou Z, Chen S, Zhou J, He X, Lv Z, Ge R, Li X, Deng T, Fodor E, Rao Z, Liu Y.** 2009. Crystal structure of an avian influenza polymerase PA(N) reveals an endonuclease active site. *Nature* **458**(7240):909–913.
57. **Biswas SK, Nayak DP.** 1994. Mutational analysis of the conserved motifs of influenza A virus polymerase basic protein 1. *Journal of Virology* **68**(3):1819–1826.
58. **Perez DR, Donis RO.** 2001. Functional analysis of PA binding by influenza A virus PB1: effects on polymerase activity and viral infectivity. *Journal of Virology* **75**(17):8127–8136.
59. **Deng T, Sharps J, Fodor E, Brownlee GG.** 2005. In vitro assembly of PB2 with a PB1-PA dimer supports a new model of assembly of influenza A virus polymerase subunits into a functional trimeric complex. *Journal of Virology* **79**(13):8669–8674.
60. **Tarendeau F, Boudet J, Guilligay D, Mas PJ, Bougault CM, Boulo S, Baudin F, Ruigrok RWH, Daigle N, Ellenberg J, Cusack S, Simorre J-P, Hart DJ.** 2007. Structure and nuclear import function of the C-terminal domain of influenza virus polymerase PB2 subunit. *Nature Structural & Molecular Biology* **14**(3):229–233.
61. **Macdonald L, Aggarwal S, Bussey KA, Desmet EA, Kim B.** 2013. Molecular interactions and trafficking of influenza A virus polymerase proteins analyzed by specific monoclonal antibodies. *Virology* **426**(1):51–59.
62. **Boivin S, Cusack S, Ruigrok RWH, Hart DJ.** 2010. Influenza A virus polymerase: structural insights into replication and host adaptation mechanisms. *Journal of Biological Chemistry* **285**(37):28411–28417.
63. **Gabriel G, Klingel K, Otte A, Thiele S, Hudjetz B, Arman-Kalcek G, Sauter M, Schmidt T, Rother F, Baumgarte S, Keiner B, Hartmann E, Bader M, Brownlee GG, Fodor E, Klenk H-D.** 2011. Differential use of importin- α isoforms governs cell tropism and host adaptation of influenza virus. *Nature Communications* **2**(156):1–7.
64. **Gabriel G, Herwig A, Klenk HD.** 2008. Interaction of polymerase subunit PB2 and NP with importin α 1 is a determinant of host range of influenza A virus. *PLOS Pathogens* **4**(2):1–10.
65. **Subbarao EK, London W, Murphy BR.** 1993. A single amino acid in the PB2 gene of influenza A virus is a determinant of host range. *Journal of Virology* **67**(4):1761–1764.
66. **Mehle A, Doudna JA.** 2009. Adaptive strategies of the influenza virus polymerase for replication in humans. *Proc Natl Acad Sci U S A* **106**(50):21312–21316.

67. **Hatta M, Hatta Y, Kim JH, Watanabe S, Shinya K, Nguyen T, Phuong SL, Quynh MLE, Kawaoka Y.** 2007. Growth of H5N1 influenza A viruses in the upper respiratory tracts of mice. *PLOS Pathogens* **3**(10):1374–1379.
68. **Pichlmair A, Sousa CR.** 2007. Review innate recognition of viruses. *Immunity* **27**(3):370–383.
69. **Yoneyama M, Fujita T.** 2008. Structural mechanism of RNA recognition by the RIG-I-like receptors. *Immunity* **29**(2):178–181.
70. **Kato H, Takahasi K, Fujita T.** 2011. RIG-I-like receptors: Cytoplasmic sensors for non-self RNA. *Immunological Reviews* **243**(1):91–98.
71. **Hornung V, Kato H, Poeck H, Akira S, Conzelmann K, Schlee M.** 2006. Ligand for RIG-I. *Science* **994**(5801):994–997.
72. **Wu B, Peisley A, Tetrault D, Li Z, Egelman EH, Magor KE, Walz T, Penczek PA, Hur S.** 2014. Molecular imprinting as a signal-activation mechanism of the viral RNA sensor RIG-I. *Molecular Cell* **55**(4):511–523.
73. **Kowalinski E, Lunardi T, McCarthy AA, Loubser J, Brunel J, Grigorov B, Gerlier D, Cusack S.** 2011. Structural basis for the activation of innate immune pattern-recognition receptor RIG-I by viral RNA. *Cell* **147**(2):423–435.
74. **Peisley A, Wu B, Yao H, Walz T, Hur S.** 2013. RIG-I forms signaling-competent filaments in an ATP-dependent, ubiquitin-independent manner. *Molecular Cell* **51**(5):573–583.
75. **Hou F, Sun L, Zheng H, Skaug B, Jiang QX, Chen ZJ.** 2011. MAVS forms functional prion-like aggregates to activate and propagate antiviral innate immune response. *Cell* **146**(3):448–461.
76. **Liu S, Chen J, Cai X, Wu J, Chen X, Wu YT, Sun L, Chen ZJ.** 2013. MAVS recruits multiple ubiquitin E3 ligases to activate antiviral signaling cascades. *Elife* **2013**(2):1–24.
77. **Woodfin BM, Kazim L.** 1993. Interaction of the amino-terminus of an influenza virus protein with mitochondria. *Archives of Biochemistry and Biophysics* **306**(2):427–430.
78. **Carr SM, Carnero E, García-Sastre A, Brownlee GG, Fodor E.** 2006. Characterization of a mitochondrial-targeting signal in the PB2 protein of influenza viruses. *Virology* **344**(2):492–508.
79. **Patel D, Schultz LW, Umland TC.** 2013. Influenza A polymerase subunit PB2 possesses overlapping binding sites for polymerase subunit PB1 and human MAVS proteins. *Virus Research* **172**:75–80.

80. **Miotto O, Heiny A, Tan TW, August JT, Brusic V.** 2008. Identification of human-to-human transmissibility factors in PB2 proteins of influenza A by large-scale mutual information analysis. *BMC Bioinformatics* **9**(1):1–18.
81. **Peisley A, Wu B, Xu H, Chen ZJ, Hur S.** 2014. Structural basis for ubiquitin-mediated antiviral signal activation by RIG-I. *Nature* **509**(7498):110–114.
82. **Barber MRW, Aldridge JR, Webster RG, Magor KE.** 2010. Association of RIG-I with innate immunity of ducks to influenza. *Proc Natl Acad Sci U S A* **107**(13):5913–5918.
83. **Sick C, Schultz U, Münster U, Meier J, Kaspers B, Staeheli P.** 1998. Promoter structures and differential responses to viral and nonviral inducers of chicken type I interferon genes. *Journal of Biological Chemistry* **273**(16):9749–9754.
84. **Childs K, Stock N, Ross C, Andrejeva J, Hilton L, Skinner M, Randall R, Goodbourn S.** 2007. mda-5, but not RIG-I, is a common target for paramyxovirus V proteins. *Virology* **359**(1):190–200.
85. **Hoffmann E, Stech J, Guan Y, Webster RG, Perez DR.** 2001. Universal primer set for the full-length amplification of all influenza A viruses. *Archives of Virology* **146**(12):2275–2289.
86. **Schaefer-Klein J, Givol I, Barsov E V, Whitcomb JM, VanBrocklin M, Foster DN, Federspiel MJ, Hughes SH.** 1998. The EV-O-derived cell line DF-1 supports the efficient replication of avian leukosis-sarcoma viruses and vectors. *Virology* **248**(2):305–311.
87. **Schwede T, Kopp J, Guex N, Peitsch MC.** 2003. SWISS-MODEL: An automated protein homology-modeling server. *Nucleic Acids Research* **31**(13):3381–3385.
88. **Altschul SF, Madden TL, Schäffer AA, Zhang J, Zhang Z, Miller W, Lipman DJ.** 1997. Gapped BLAST and PSI-BLAST: A new generation of protein database search programs. *Nucleic Acids Research* **25**(17):3389–3402.
89. **Remmert M, Biegert A, Hauser A, Söding J.** 2011. HHblits: lightning-fast iterative protein sequence searching by HMM-HMM alignment. *Nature Methods* **9**(2):173–175.
90. **Westbrook J, Feng Z, Chen L, Yang H, Berman HM.** 2003. The protein data bank and structural genomics. *Nucleic Acids Research* **31**(1):489–491.
91. **Reich S, Guilligay D, Pflug A, Malet H, Berger I, Crépin T, Hart D, Lunardi T, Nanao M, Ruigrok RWH, Cusack S.** 2014. Structural insight into cap-snatching and RNA synthesis by influenza polymerase. *Nature* **516**(7531):361–366.

92. **Waterhouse AM, Procter JB, Martin DMA, Clamp M, Barton GJ.** 2009. Jalview Version 2-A multiple sequence alignment editor and analysis workbench. *Bioinformatics* **25**(9):1189–1191.
93. **Schindelin J, Arganda-Carreras I, Frise E, Kaynig V, Longair M, Pietzsch T, Preibisch S, Rueden C, Saalfeld S, Schmid B, Tinevez JY, White DJ, Hartenstein V, Liceiri K, Tomancak PAC.** 2012. Fiji: an open source platform for biological image analysis. *Nature Methods* **9**(7):676–682.
94. **Miranzo-Navarro D, Magor KE.** 2014. Activation of duck RIG-I by TRIM25 is independent of anchored ubiquitin. *PLOS One* **9**(1):1–12.
95. **Xu H, He X, Zheng H, Huang LJ, Hou F, Yu Z, de la Cruz MJ, Borkowski B, Zhang X, Chen ZJ, Jiang QX.** 2014. Structural basis for the prion-like MAVS filaments in antiviral innate immunity. *Elife* **2014**(3):1–25.
96. **Berke IC, Li Y, Modis Y.** 2013. Structural basis of innate immune recognition of viral RNA. *Cell Microbiology* **15**(3):386–394.
97. **Rawling DC, Pyle AM.** 2014. Parts, assembly and operation of the RIG-I family of motors. *Current Opinion in Structural Biology* **25**:25–33.
98. **Lu A, Magupalli V, Ruan J, Yin Q, Maninjay K, Vos M, Schröder GF, Fitzgerald KA, Wu H, Egelman EH.** 2014. Unified polymerization mechanism for the assembly of ASC-dependent inflammasomes. *Cell* **156**(6):1193–1206.
99. **Liniger M, Moulin HR, Sakoda Y, Ruggli N, Summerfield A.** 2012. Highly pathogenic avian influenza virus H5N1 controls type I IFN induction in chicken macrophage HD-11 cells: a polygenic trait that involves NS1 and the polymerase complex. *Virology Journal* **9**(1):1–9.
100. **Doyle RJ, Lee NC.** 1986. Microbes, warfare, religion, and human institutions. *Canadian Journal of Microbiology* **32**(3):193–200.
101. **Steinhauer DA, Holland JJ.** 1987. Rapid evolution of RNA viruses. *Annual Review Microbiology* **41**:409–433.
102. **Ewald PW.** 1983. Host-parasite relations, vectors, and the evolution of disease severity. *Annual Reviews Ecological and Systematics* **14**:465–485.
103. **Anderson RM, May RM.** 1982. Coevolution of hosts and parasites. *Parasitology* **85**:229–239.
104. **Fraser C, Hollingsworth TD, Chapman R, de Wolf F, Hanage WP.** 2007. Variation in HIV-1 set-point viral load: epidemiological analysis and an evolutionary hypothesis. *Proc Natl Acad Sci U S A* **104**(44):17441–17446.

105. **To KK-W, Zhou J, Chan JF-W, Yuen K-Y.** 2015. Host genes and influenza pathogenesis in humans: an emerging paradigm. *Current Opinion in Virology* **14**:7–15.
106. **Gygi SP, Rochon Y, Franza BR, Aebersold R.** 1999. Correlation between protein and mRNA abundance in yeast. *Molecular and Cellular Biology* **19**(3):1720–1730.
107. **Van Hoesen N, Pappas C, Belser JA, Maines TR, Zeng H, García-Sastre A, Sasisekharan R, Katz JM, Tumpey TM.** 2009. Human HA and polymerase subunit PB2 proteins confer transmission of an avian influenza virus through the air. *Proc Natl Acad Sci U S A* **106**(9):3366–3371.